

A Statistical Analysis of Compositional Surveys

Michelle Pistner Nixon¹², Jeffrey Letourneau³, Lawrence A. David ³⁴,
 Sayan Mukherjee⁴⁵, and Justin D. Silverman¹²⁶⁷

Abstract

In the analysis of modern sequencing data, a common statistical problem is inference from positive-valued multivariate measurements where the scale (e.g., sum) of the measurements are not representative of the scale (e.g., total size) of the system being studied. The field of Compositional Data Analysis (CoDA) axiomatically forces analyses to be invariant to scale, yet scientific questions often rely on the unmeasured system scale for identifiability. Instead, many existing tools make a variety of assumptions to identify models, often imputing the unmeasured scale. We analyze the theoretical limits on inference and formalize the assumptions required to provide principled scale reliant inference. Using statistical concepts such as consistency and calibration, we provide guidance on how to make scale reliant inference from these data. We prove that the Frequentist ideal is often unachievable and that existing methods can demonstrate bias and a breakdown of Type-I error control. We introduce scale simulation estimators and scale sensitivity analysis as a rigorous, flexible, and computationally efficient means of performing scale reliant inference.

Keywords: Multivariate Analysis, Identifiability, Uncertainty Quantification, Sequence Count Data

¹Equal contributions

²College of Information Sciences and Technology, Pennsylvania State University

³Department of Molecular Genetics and Microbiology, Duke University

⁴Center for Genomic and Computational Biology, Duke University

⁵Departments of Statistical Science, Mathematics, Computer Science, Biostatistics & Bioinformatics, Duke University

⁶Departments of Statistics and Medicine, Pennsylvania State University

⁷Corresponding author: JustinSilverman@psu.edu

1 Introduction

Many scientific fields collect noisy, multivariate, positive-valued data to profile the abundances of distinct classes in an underlying system of interest. For example, in ecology, researchers measure species abundances to identify factors which structure ecosystems. This paper studies the case where limitations of the measurement process cause the scale of each measurement (e.g., the total number of counted animals) to misrepresent the scale of the system being studied (e.g., the actual number of animals). Even in the absence of measurement noise, these data only provide information about the proportional abundances of the different classes. There are at least two distinct approaches to modeling such data; we call these the Compositional Data Analysis (CoDA) and imputation approaches.

CoDA axiomatically restricts inference to quantities that can be identified by proportional abundances. This is often called the axiom of scale invariance (Pawlowsky-Glahn et al., 2015b, pg. 12). Though intuitive, this axiom can be limiting: proportional abundances alone are insufficient to express some scientific questions that rely on the scale of the system (Jarauta Bragulat et al., 2011). CoDA provides a very limited suite of tools for answering such scale reliant questions (Pawlowsky-Glahn et al., 2015a; Martín-Fernández et al., 2021), and even those methods assume that the scale is known or measured directly. Instead, CoDA often suggests that researchers change their question to be identifiable given the observed data (e.g., Lovell et al. (2015)). Unsurprisingly, many researchers find this approach unsatisfying and turn to the imputation approach.

The imputation approach imposes identifiability on scale reliant questions with a variety of either explicit or implicit assumptions that, in effect, impute the missing scale information from the observed data. Examples include data normalizations (Kurtz et al., 2015; Love et al., 2014), penalized estimation (Friedman and Alm, 2012; Fang et al., 2015), or models that assume conditional independence in the measurement process (Love et al., 2014; Choi et al., 2017; Chiquet et al., 2021). Experimental limitations often prevent direct

validation of these assumptions. Intuition and experience mitigate this restriction by identifying cases where these assumptions cannot hold. For example, authors have argued that data normalizations developed for bulk RNA-seq gene expression studies may be invalid for some microbiome datasets (Love, 2021). Still, these guidelines remain qualitative and do not quantify how errors in identifying assumptions impact study conclusions.

Motivated by the limitations of both the CoDA and imputation approaches, we develop new theory and methods for what we term *scale reliant inference*: inference of quantities that require knowledge of the scale of the system under study. The main contributions of this article are five-fold. First, we introduce compositional surveys as a probabilistic reformulation of compositional data which allows us to replace axiomatic foundations of CoDA with more established statistical criteria such as consistency and calibration. Through this approach, we prove the non-existence of consistent point estimators and calibrated confidence sets for some of the most commonly performed analyses of compositional surveys. Second, given these limits on inference, we study the role of identifying assumptions on inference. We find that many of the most common identifying assumptions implicitly assume infinite knowledge in the system scale, leading to an unacknowledged bias. We show both theoretically and empirically that this bias can cause existing methods to demonstrate increasing type-I error rate with increasing sample size. Third, we mitigate these limitations of existing methods by accounting for potential error within identifying assumptions. We introduce the scale simulation framework as a flexible and computationally efficient approach to performing scale reliant inference. Fourth, we demonstrate how to check the assumptions made during scale simulation through sensitivity analyses. Contrary to the axioms of CoDA, we successfully apply principled scale reliant inference of compositional surveys to both real and simulated data. Finally, with application to sequence count data, this work provides a new framework for discussions about the possibilities and limitations of that data.

The remainder of this introduction explores a motivating example based on the analysis of human oral microbiota, describes the ALDEx2 model which will serve as a prototypical example of a microbiome analysis, and clarifies terminology.

1.1 A Motivating Example

The human mouth contains hundreds to thousands of distinct bacterial taxa which play critical roles in host physiology and pathology. For a population of size N , we represent the microbiota in a population as an $N \times D$ ecosystem W with elements W_{ij} representing the abundance of taxa $i \in \{1, \dots, D\}$ in the mouth of subject $j \in \{1, \dots, N\}$. As we cannot directly observe and measure microbiota, we approximate using high-throughput DNA sequencing (e.g., 16S rRNA amplicon sequencing). This results in data Y with elements Y_{ij} representing the number of observed DNA molecules which map to taxa i from subject j . The total number of sequences $Y_j^\perp = \sum_i Y_{ij}$ is a feature of the measurement process and does not reflect the total microbial load in the mouth of subject j ($W_j^\perp = \sum_i W_{ij}$) (Morton et al., 2019). However, important biomedical questions depend on the microbial load. For example, identifying individual taxa that increase or decrease in abundance between conditions (often referred to as differential abundance analysis) could help identify the mechanisms underlying diseases (e.g., Verma et al. (2018)). Differential abundance analysis can be framed, for each taxa i , as the expected log-fold change: $\theta_i = \mathbb{E}[\log(W_{i(case)}/W_{i(control)})]$ (Morton et al., 2019). Differential abundance can be rewritten as

$$\theta_i = \mathbb{E} \left[\log \frac{W_{i(case)}^{\parallel}}{W_{i(control)}^{\parallel}} \right] + \mathbb{E} \left[\log \frac{W_{(case)}^{\perp}}{W_{(control)}^{\perp}} \right], \quad (1)$$

where the notation W^{\parallel} denotes the proportional abundances. Clearly, differential abundance depends on the unmeasured scale of the system (W^{\perp}), and it is therefore not a scale invariant quantity as CoDA advises. In fact, unless these expectations are taken with

respect to a singular probability model that implies a deterministic relationship between W^\perp and W^\parallel , θ_i is not identifiable from the observed data.

Recognizing the disconnect between the information content of the observed data and the scientific question of interest, current methods often use data normalization, variance stabilizing transforms, or generative models that aim to impute the missing scale information (see Jeganathan and Holmes (2021) and McMurdie and Holmes (2014) for a thorough discussion of current best practices with application to microbiota). In all cases, these methods make assumptions to create or impute a surrogate for the missing scale information. As an example, we focus on the ALDEx2 model, which uses a centered log-ratio parameter transformation for differential abundance analysis (Fernandes et al., 2014). We highlight ALDEx2 for its popularity and the simplicity of its model, which simplifies our discussion. While the ALDEx2 library has grown over time, for brevity we discuss ALDEx2 as originally published:

$$\begin{aligned} Y_{\cdot j} &\sim \text{Multinomial}(\phi^{-1}(\eta_{\cdot j})) \\ \phi^{-1}(\eta_{\cdot j}) &= W_{\cdot j}^\parallel \\ W_{\cdot j}^\parallel &\sim \text{Dirichlet}(\gamma) \end{aligned}$$

where γ are prior parameters and ϕ denotes the Centered Log-Ratio (CLR) transform $\eta_{\cdot j} = \log \left[W_{ij}^\parallel / g(W_{\cdot j}^\parallel) \right]$. Posterior samples of η are used to evaluate the null hypothesis $\mathbb{E}[\eta_{i(x=1)} - \eta_{i(x=0)}] = 0$ for conditions $x_j \in \{0, 1\}$, over the posterior using a t-statistic or Wald-type statistic. The results are then summarized with a p-value like statistic.¹

The CLR normalization is actually one of the three data transforms at the heart of CoDA. The CLR transform is scale invariant: $\phi(W_{\cdot j}) = \phi(W_{\cdot j}^\parallel)$. In fact, ALDEx2 is scale invariant; changes in W^\perp do not influence estimates of η . Yet some tasks performed by

¹While it is called a p-value by the authors, it is not a true p-value due to the dependence on the prior hyperparameter γ .

ALDEx2, namely estimation of differential abundance, are scale reliant. We propose that this seeming-paradox arises from assumptions used in model interpretation. Consider that ALDEx2 does not evaluate the log-fold change of W ; instead, it evaluates the difference in η which can be expressed as:

$$\mathbb{E}[\eta_{i(x=1)} - \eta_{i(x=0)}] = \mathbb{E} \left[\log \frac{W_{i(x=1)}^{\parallel}}{W_{i(x=0)}^{\parallel}} \right] + \mathbb{E} \left[\log \frac{g(W_{\cdot(x=0)}^{\parallel})}{g(W_{\cdot(x=1)}^{\parallel})} \right]. \quad (2)$$

Still, the difference in η is often interpreted as differential abundance (Fernandes et al., 2014). The only way these two are equivalent is under the implicit assumption that

$$\Delta \equiv \mathbb{E} \left[\log \frac{g(W_{\cdot(x=0)}^{\parallel})}{g(W_{\cdot(x=1)}^{\parallel})} \right] - \mathbb{E} \left[\log \frac{W_{\cdot(x=1)}^{\perp}}{W_{\cdot(x=0)}^{\perp}} \right] = 0, \quad (3)$$

i.e., that the scales can be recovered from the geometric mean of the compositions. What remains unclear is the sensitivity of ALDEx2 to errors in this assumption. In Section 4.2 we show that both ALDEx2 (and another popular model DESeq2) can lead to false discovery rates on the order of 80% with only slight deviations from their implicit assumptions.

1.2 A Clarification: Totals versus Scales

Throughout much of the CoDA literature, the term *total* is used interchangeably with the term *scale*, as all analyses are axiomatically scale invariant. But as our present focus is on scale reliant inference, the distinction is non-trivial. For us, the total is an example of a scale; the relevant scale is often study-specific. Consider two researchers conducting independent human oral microbiome studies who both aim to infer differential abundance between case and control groups: $\theta_i = \mathbb{E}[\log(W_{i(case)}/W_{i(control)})]$. One researcher may be interested in identifying which taxa change in absolute abundance between cases and controls, so for her W_{ij} represents the total number of bacteria of species i in the mouth of subject j . With this specification of W , W_j^{\perp} then represents the total number of bacteria

of any type in the mouth of subject j (the total scale). But the other researcher may be uninterested in changes in absolute abundance and prefer to study the concentration of microbes (e.g., cells/mL) with W_j^\perp representing the total concentration of bacteria in the mouth of subject j . For concreteness and brevity, we use the total scale in discussions. However, our methods and conclusions can be applied to any relevant scientific scale.²

2 Limits on Inference with Compositional Surveys

In the prior section, we highlighted the challenge of scale reliant inference by framing the issue in terms of parameter identifiability. Here, we formalize that viewpoint for a more thorough investigation on the limits of inference. First, we review the definition of compositional data to motivate the need for a new approach.

Compositional data are defined as positive, multivariate data that sum to a constant value, e.g., measurements x such that $0 < x_i < 1$ for all i and $\sum_i x_i = k$ for some constant k which is termed the scale of the composition (Aitchison, 1982). This definition is not rich enough to support a study of the limits of inference: with no mention of the system being studied, we lack the theoretical tools needed to investigate when an analysis will faithfully represent the underlying state of nature. Moreover, we find this definition overly restrictive as many data that lack scale (e.g., sequence count data) are neither continuous nor sum to a constant value. We address both limitations: our new formulation focuses less on the mathematical structure of the observed data and more on the limited information that the measurements provide about an underlying system of interest.

²This idea of scales is a generalization of the idea of reference frames (Morton et al., 2019). In the special case where a scale is based on a feature internal to the composition of a system under study (e.g., the geometric mean of the composition), scales can be thought of as the inverse of reference frames.

2.1 Definitions and Foundations

2.1.1 Scaled Systems and Scale Reliance

We define compositional surveys starting from the underlying system of interest – a scaled system. Scaled systems formalize the notion of a system that is made up of distinct classes of elements combined in potentially differing amounts.

Definition 1 (Scaled System). *A scaled system \mathcal{W} is a D -dimensional positive-valued stochastic process over a set of conditions $m \in \mathbf{M}$. The scale of \mathcal{W} is defined point-wise as $\mathcal{W}(m)^\perp = \sum_i \mathcal{W}_i(m)$. The composition of \mathcal{W} is defined point-wise for each condition $m \in \mathbf{M}$ by*

$$\mathcal{W}(m)^\parallel = (\mathcal{W}_1(m)/\mathcal{W}(m)^\perp, \dots, \mathcal{W}_D(m)/\mathcal{W}(m)^\perp).$$

That is, a scaled system can be decomposed as $\mathcal{W}(m) = \mathcal{W}(m)^\parallel \mathcal{W}(m)^\perp$.

The System Existence and Interest Assumption We assume the existence of a scaled system. Further, we assume that this system is of central scientific interest such that the goals of a study can be framed in terms of a probability model $P_\theta(\mathcal{W})$, called the target model with θ the parameter of interest. The target model represents the model a researcher would use given direct observations of \mathcal{W} . That is, we assume that there exists a scientific question of interest specific enough to specify a target model.

We next characterize target models based on whether they require knowledge of \mathcal{W}^\perp to identify θ . We distinguish between three types of model identifiability: identifiable, partially unidentifiable, and fully unidentifiable.

Definition 2 (Identification Region). *For a random variable Z and parameter $\theta \in \Theta$ related through a probability model of the form $P_\theta(Z)$, the identification region of θ is*

$$Id_\theta(Z) = \tilde{\Theta} : \{\tilde{\Theta} \subseteq \Theta, \forall \theta_i, \theta_j \in \tilde{\Theta}, P_{\theta_i}(Z) = P_{\theta_j}(Z)\}.$$

θ is identifiable if $Id_\theta(Z)$ is a singleton set. If $Id_\theta(Z) \subset \Theta$, then θ is partially unidentified. If $Id_\theta(Z) = \Theta$, then θ is fully unidentified.

Definition 3 (Scale Reliant Parameter). *Scale reliance is defined for a target model $P_\theta(\mathcal{W})$ in terms of the identifiability of θ with respect to \mathcal{W}^\parallel . If $Id_\theta(\mathcal{W}^\parallel)$ is a singleton set, the target model is scale invariant. If $Id_\theta(\mathcal{W}^\parallel) \subset \Theta$, the target model is partially scale reliant. If $Id_\theta(\mathcal{W}^\parallel) = \Theta$, the target model is fully scale reliant.*

Intuitively, fully scale reliant means even perfect knowledge of \mathcal{W}^\parallel is not enough to restrict possible values of θ .

2.1.2 Compositional Surveys

We next introduce compositional surveys as a measurement of a scaled system.

Definition 4 (Compositional Survey). *Let \mathbf{W}^\perp denote the set of all possible system scales defined over a set of conditions \mathbf{M} . A compositional survey \mathcal{Y} of a scaled system \mathcal{W} is a D -dimensional positive-valued stochastic process that identifies the composition of the system ($Id_{\mathcal{W}^\parallel}(\mathcal{Y})$ is a singleton set) but does not identify the scale of the system ($Id_{\mathcal{W}^\perp}(\mathcal{Y})$ is not a singleton set). We distinguish between partial compositional surveys $Id_{\mathcal{W}^\perp}(\mathcal{Y}) \subset \mathbf{W}^\perp$ and full compositional surveys $Id_{\mathcal{W}^\perp}(\mathcal{Y}) = \mathbf{W}^\perp$.*

Unlike compositional data, our definition of compositional surveys is solely a statement of the limited information content that the data can provide about the underlying system of interest. We next connect compositional surveys to the parameter of interest θ . A proof of the following statement can be found in Supplementary Section A.1.

Proposition 1. *Let \mathcal{Y} denote a fully compositional survey of a scaled system \mathcal{W} . If the target model $P_\theta(\mathcal{W})$ is scale reliant, then θ is partially unidentified by \mathcal{Y} . If the target model is fully scale reliant, then θ is fully unidentified by \mathcal{Y} .*

2.1.3 Assumptions

The framework above is quite general, with few restrictions on the target model, on the measurement model of the compositional survey, or even on the sample space of the compositional survey and scaled system. Still, to avoid needlessly complicating our later discussions, we introduce three assumptions to exclude trivialities and ensure focus on the complexities of real science.

The Non-Singular Uncertainty Assumption We assume that, in the absence of any data, there remains non-singular uncertainty over \mathcal{W} . Thus if a target model is scale reliant, performing inference using only a compositional survey includes a potential for error.

The Irreducible Scale Assumption We assume that if a parameter θ is defined with respect to \mathcal{W}^\perp (e.g., Equation 1) and cannot be expressed solely in terms of \mathcal{W}^\parallel , then the target model $P_\theta(\mathcal{W})$ is not expressible in a reduced form $P_\theta(\mathcal{W}^\parallel)$. This assumption simplifies our discussion, so we can refer to whether a parameter is scale reliant without discussing all possible target models expressing that parameter. This assumption could be violated if a researcher had *a priori* knowledge of a fixed relationship $\mathcal{W}^\perp = h(\mathcal{W}^\parallel)$. We expect this does not occur frequently in practice.

The Noisy Data Assumption For any partially compositional survey, we assume that the measurement noise is large enough that, in the finite data regime, the survey is well approximated as a fully compositional survey. Under this assumption, imputing the scale from survey data is not possible when working with compositional surveys. We discuss this assumption in more detail in Supplementary Section A.2.

2.1.4 Application to Sequence Counting

We briefly demonstrate the applicability of these definitions by relating them to differential and correlation analyses. It follows from Equation (1) that differential analysis is fully scale reliant under the Irreducible Scale Assumption. In Supplementary Section A.3, we show that correlation analysis, defined in terms of parameters $\theta_i = \text{Cor}(\log \mathcal{W}_i, \log \mathcal{W}_j)$, is also fully scale reliant. With the Noisy Data Assumption, this implies that both differential and correlation analyses are fully unidentifiable using a full compositional survey or a partially compositional survey. Combined with recent evidence that sequence counting does not retain information on the system under study Vandeputte et al. (2017), this suggests that these analyses are fully unidentified by sequence count data. In fact, even if the noisy data assumption is invalid for sequence count data, these analyses may still be fully unidentifiable (see Supplementary Section A.2 for further discussion).

3 Consistency and Calibration

All forms of statistical inference rely on certain criteria for validity. Frequentist inference centers on the existence of consistent estimators and calibrated confidence sets. By focusing on these criteria and viewing scale reliant inference as a challenge of identifiability, we can provide new insights into the limits of inference with compositional surveys. Our main result shows that, with only a compositional survey, inference of fully scale reliant parameters cannot satisfy these core Frequentist criteria.

We next define a min- ρ sequence of estimators in order to provide a definition of estimator consistency. We define a min- ρ sequence of compositional surveys as a two dimensional sequence indexed by the tuple (ρ, s) such that the minimum s denotes the set of conditions surveyed ($s \subset \mathbf{M}$) and $\rho = \text{Inf}_{s \in \mathbf{S}} r_s$ denotes the minimum number of observations obtained at any one condition in the survey. Intuitively, as $\rho \rightarrow \infty$ and $s \rightarrow \mathbf{M}$, this sequence

accesses as much information about the distribution of \mathcal{W} as could be obtained from a compositional survey \mathcal{Y} . We define a min- ρ sequence of estimators as a sequence obtained by applying an estimator $\hat{\theta}$ to a min- ρ sequence of compositional surveys. With these definitions, we can define estimator consistency in the context of compositional surveys.

Definition 5 (Consistent Estimators). *Let $\{\hat{\theta}^{(\rho,s)}\}$ denote a min- ρ sequence of estimators for a parameter θ based on a compositional survey \mathcal{Y} . $\hat{\theta}$ is a consistent estimator of θ if and only if, for all $\epsilon > 0$,*

$$\lim_{\rho \rightarrow \infty, s \rightarrow \mathbf{M}} P(||\hat{\theta}^{(\rho,s)} - \theta|| \leq \epsilon) = 1.$$

We can now state a key result: the non-existence of consistent point estimators. We provide a proof in Supplemental Section A.1.

Theorem 1. *Let \mathcal{Y} denote a fully compositional survey or a partially compositional survey under the noisy data assumption. If $\theta \in \Theta$ is a scale reliant parameter, then there does not exist a sequence of estimators $\{\hat{\theta}^{(\rho,s)}\}$ based on \mathcal{Y} that is consistent.*

Given that differential abundance and correlation analysis are scale reliant parameters, this result implies that there does not exist a consistent estimator for either of these two popular inference tasks using sequence count data.

Still, non-existence of consistent point estimation is not unmanageable: a calibrated set estimator (i.e., confidence set) may suffice for Frequentist inference. Remarkably, prior studies have successfully developed calibrated confidence sets for unidentified parameters (e.g., Imbens and Manski (2004)). Yet these works studied situations in which the parameter of interest was partially unidentified, rather than fully unidentified. To provide new results for fully unidentified parameters, we must first introduce the notion of a usable calibrated confidence set, which excludes the possibility of trivial sets (e.g., the set of all possible parameter values).

Definition 6 (Usable Calibrated Confidence Set). *For an unknown parameter $\theta \in \Theta$ related to the unknown population P_θ , a set estimator $S(X) \subset \Theta$ is a confidence set calibrated at level β if*

$$\inf_{\theta \in \Theta} P_\theta(\theta \in S(X)) \geq \beta. \quad (4)$$

$S(X)$ is a usable confidence set if $S(X)$ is a calibrated confidence set at level β satisfying two additional requirements: (1) $\beta > 0$ and (2) for any $\theta_i \in \Theta$, there exist some $\theta_j \in \Theta$ such that $P_{\theta_i}(\theta_j \notin S(X)) = 1$.

We can now state a major result of this work. The proof of the following theorem is provided in Supplementary Section A.1.

Theorem 2. *If $\theta \in \Theta$ is fully unidentifiable given a random variable X , then there does not exist a usable confidence set of the form $S(X)$.*

Corollary 1. *If \mathcal{Y} is either a fully compositional survey or a partially compositional survey under the Noisy Data Assumption, then there does not exist a usable calibrated confidence set $S(\mathcal{Y})$ for a fully scale reliant parameter.*

This is a startling result. For example, it implies that with sequence count data alone, there does not exist a (non-trivial) hypothesis test for the standard definition of differential abundance or correlation analysis that is calibrated at level $\beta > 0$.³ The contrapositive states that if a calibrated confidence set exists, then sequence count data is only a partial compositional survey and the noisy data assumption is not valid. Even with a usable calibrated confidence set, θ would still (except in trivial cases) be only partially identified, invalidating commonly used Frequentist estimators and requiring specialized tools such of those proposed in Imbens and Manski (2004).

³Trivially, a hypothesis test that only tests whether the true differential abundance exists between negative and positive infinity would be calibrated and would control Type-I error.

Why then do so many methods that perform fully scale reliant inference (e.g., differential analysis) claim to be calibrated in a Frequentist sense (Love et al., 2014; Fernandes et al., 2014; Srinivasan et al., 2020)? Perhaps these methods are not interested in changes in scaled abundances but tautologically aim to draw inference from their exact model; i.e., methods that use normalization for identifiability truly aim to infer changes in the normalized abundances. We find this answer unsatisfying as, in our experience, normalization methods are often chosen for convenience or favorable mathematical properties; it does not exactly match with the scientific question of interest. Another possibility is to view existing claims of Frequentist calibration with healthy skepticism, noting that these methods may only be calibrated in restricted settings that are consistent with their own assumptions. For example, Srinivasan et al. (2020) uses simulation to claim Type-I error control but do so using Multinomial-Dirichlet simulations which are trivially identified by a compositional survey. Others such as Hawinkel et al. (2019) have echoed this sentiment, noting a “self-fulfilling prophecy” of papers that claim calibration with hand-picked simulations.

4 Inference Under Assumptions

The prior section proved that many common analyses of compositional surveys (i.e., fully scale reliant analyses) cannot achieve the Frequentist ideal. Also, many methods impose additional assumptions to uniquely identify parameter estimates. To study the impact of violations of these assumptions, we borrow the concept of unacknowledged bias from the field of partially identified models (Gustafson, 2015). Beyond Frequentist inference, we also use unacknowledged bias to understand the limitations of existing Bayesian approaches to scale reliant inference. Before introducing unacknowledged bias, we introduce a formal definition of identifying restrictions to examine current methods.

4.1 Identifying Restrictions

Definition 7. *Identifying restrictions are singular probabilistic models defined over the set of all possible scales \mathbf{W}^\perp . That is, a model $p(\mathcal{W}^\perp)$ is an identifying restriction if $\text{Det} |\text{Var}[p(\mathcal{W}^\perp)]| = 0$ where $\text{Det} |\cdot|$ denotes the determinant.*

Many popular methods of scale reliant inference use identifying restrictions. For example, the ALDEx2 model (see Section 1.1) assumes that differential changes in CLR coordinates are equal to differential changes in scaled abundances. This assumption can be captured in a scale model of the form $p(\mathcal{W}^\perp) = [\delta(\mathcal{W}(j)^\perp = 1/g(\mathcal{W}(j)^\parallel))]$ for all j] where $\delta(x)$ denotes a point mass at x . This scale model has zero variance and is therefore an identifying restriction.

Many other methods use the same identifying restriction: they equate changes in CLR coordinates with changes in scaled abundances (Kurtz et al., 2015; Srinivasan et al., 2020). In fact, the same logic shows that any analyses equating changes in normalized or transformed sequence count data to changes in scaled abundances implicitly use some form of identifying restriction. Even some penalized estimators represent identifying restrictions (see Supplementary Section A.3 for an example). In the next subsection, we motivate how identifying restrictions can cause problems.

4.2 Unacknowledged Bias

Following Gustafson (2015), we say an estimator displays an unacknowledged bias if it is biased but does not account for that bias through its variance. For example, an estimator whose asymptotic variance tends to zero despite having a large-sample bias displays an unacknowledged bias. Estimators that display unacknowledged bias can lead to inappropriate certainty in an incorrect result.

Identifying restrictions, can lead to an unacknowledged bias in scale reliant inference.

We provide an intuitive explanation. Under the non-singular uncertainty assumption, a researcher's true uncertainty about the unmeasured system scale covers some non-degenerate set $\mathbf{w}^\perp \in \mathbf{W}^\perp$. Yet, by Definition 7, any identifying restriction places non-zero probability on only an infinitesimal (i.e., degenerate) portion of \mathbf{w}^\perp and therefore has an infinitesimal probability of accurately capturing the true scale of interest. As the inference is scale reliant, the chosen identifying restriction also restricts the set of possible values of the parameter θ . We denote the restricted set Θ_R and the full set Θ . In fact, the probability that the true value of θ exists in Θ_R is largely a feature of the cardinality of Θ : if Θ is an infinite set, the probability that θ exists in Θ_R is infinitesimal and the probability of bias is essentially 1. Assuming standard parametric theory applies to the chosen estimator, the asymptotic variance of the estimator will tend to zero, leading to an unacknowledged bias.

Estimators with unacknowledged bias often perform worse with more data. With few samples, uncertainty from the sampling model can cover the estimator bias. But with increasing sample sizes, this sampling variation often disappears, resulting in an unacknowledged bias.

We demonstrate this phenomenon in Figure 1: we simulate a microbial community consisting of 21 taxa. Treatment with a mild antibiotic produces a slight decrease in the abundance of 4 of the 21 taxa. For a sample size of n equally split between the Pre-Antibiotic ($x = 0$) and Post-Antibiotic ($x = 1$) groups, we simulated the true abundance of each taxa i according to $\text{Poisson}(\lambda_{ix_j})$. To simulate the loss of scale information, we re-sampled the data to an arbitrary scale (see Supplementary Section B). We then applied ALDEx2 and DESeq2 to the re-sampled data. Notably, we designed this simulation to only slightly deviate from ALDEx2's identifying restriction: we chose λ such that $\Delta = 0.1$ (see Eq. 3). We also expected this to slightly deviate from the identifying restriction used by DESeq2 (a median of ratios normalization), which can roughly be thought of as a non-parametric analogue of the CLR normalization (Quinn et al., 2018, Supplement).

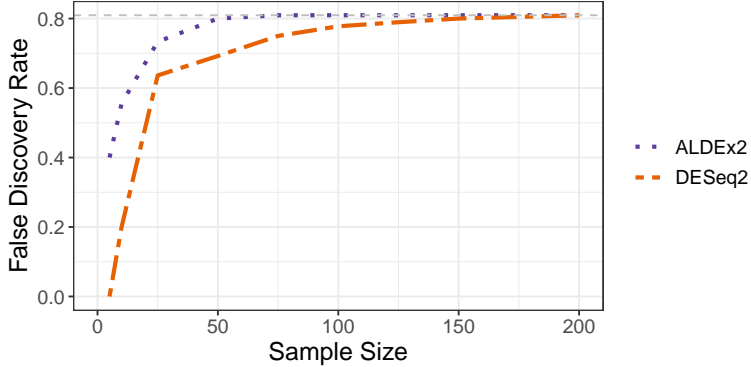


Figure 1: False discovery rate versus sample size for ALDEx2 and DESeq2. For each method, false discovery rate increases even in the presence of infinite data. The maximum false discovery rate was 0.81, as four of 21 taxa were truly differentially expressed. Sequencing depth was set to 5,000. Simulation details are in Supplementary Section B.

Figure 1 shows the expected behavior; the false discovery rate of both methods increased as a function of the number of observations (n) to a maximum of 0.81, which corresponds to calling every taxa differentially abundant.

4.3 Bayesian Methods

The above results suggest that identifying restrictions are limited because they ignore potential uncertainty or error in their assumptions regarding scale. Combined with our results in Section 3, where we proved that the Frequentist ideal of calibration cannot be attained for fully scale reliant problems, this limitation supports alternative inference paradigms that incorporate subjective uncertainty into analyses and have less stringent inferential criteria. Bayesian inference is the natural choice, where we specify uncertainty in scale with a prior distribution. Indeed, the distinct notions of calibration in Bayesian inference make no requirements on model identifiability (Neath and Samaniego, 1997), only that the prior accurately reflects belief and that the likelihood function faithfully

represents the information content of the data (i.e., the law of likelihood). Still, in moving to a Bayesian perspective, we must relax our criteria for inference to consider notions such as consistency or calibration of set estimators. Whereas the Frequentist notion of calibration represents a guarantee of nominal coverage even in the worst case (i.e., infimum over all possible θ in Eq. 4), Bayesian calibration is a weaker guarantee of expected nominal coverage with expectation taken with respect to the prior distribution (Gustafson, 2015, pg. 41). Still, Bayesian inference is clearly useful and the limitations of the Frequentist perspective motivate a Bayesian approach for scale reliant inference.

However, many Bayesian methods used for scale reliant inference demonstrate unacknowledged bias. In order to satisfy the law of likelihood, the likelihood of a Bayesian model must acknowledge any non-identifiability by updating only those parts of the prior which are informed by the observed data (Gustafson, 2015). Models with a likelihood that update only a portion of the prior are termed Bayesian Partially Identified Models (Bayesian PIMs, Gustafson (2015)). In the analysis of sequence count data, we are aware of only one Bayesian model that satisfies this property (Schwager et al., 2017). More commonly, models used for scale reliant inference assume some independence between the sequences, e.g., using product Poisson or Negative Binomial models (e.g., (Pendegraft et al., 2019)). Following standard parametric theory, in the asymptotic limit, the posterior of these models converge to a point mass centered at their maximum likelihood estimate. Based on our previous discussion, it is clear that this will be a biased point estimator with probability 1, i.e., these models display an unacknowledged bias. In contrast, by updating only the portion of the prior that is actually identified by the observed data, Bayesian PIMs can remain calibrated and acknowledge their potential bias through a variance that remains non-zero even in the asymptotic limit. In the next section, we discuss the potential application and generalization of Bayesian PIMs for the analysis of compositional surveys.

5 Scale Simulation

Bayesian PIMs can mitigate unacknowledged bias by accounting for uncertainty in the assumptions used to identify inference (Gustafson, 2015, pg. 36). As we framed compositional surveys in terms of model identifiability, it is natural to develop Bayesian PIMs for scale reliant inference. However, two features of Bayesian PIMs limit their applicability in practice. First, these models can be computationally challenging to infer secondary to highly anisotropic posterior distributions which arise from a likelihood that only updates a subset of the prior. These models often require highly specialized inference algorithms and may not scale to high dimensional problems. Second, highly specialized inference algorithms come with an added restriction on types of priors that can be specified (Gustafson, 2015, pg. 24). We seek an efficient and flexible approach to scale reliant inference to easily specify uncertainty over the unmeasured scales without restricting to a particular functional form for that uncertainty. We introduce scale simulation estimators to address this challenge. We prove that these estimators are a generalization of Bayesian PIMs, and share critical calibration properties that help alleviate unacknowledged bias.

Scale simulation starts with a *target estimand*. Unlike standard estimands such as the mean or variance of a population, the target estimand is itself an estimator of the parameter of interest θ based on a scaled system, i.e., $\hat{\theta} = f(\mathcal{W}^{\parallel}, \mathcal{W}^{\perp})$. The target estimand is specified, not in terms of available data, but with respect to the desired complete data. Scale simulation accounts for our uncertainty in the complete data. We highlight two sources of uncertainty: in \mathcal{W}^{\perp} and in \mathcal{W}^{\parallel} . Starting with the latter, we can specify a measurement model $p(\mathcal{W}^{\parallel}|\mathcal{Y})$ and then construct a *conditional estimand* $f(\mathcal{W}^{\perp}, \mathcal{Y}) = \mathbb{E}_{p(\mathcal{W}^{\parallel}|\mathcal{Y})} f(\mathcal{W}^{\parallel}, \mathcal{W}^{\perp})$ which incorporates uncertainty in \mathcal{W}^{\parallel} into the target estimand. Second, we specify a *scale model* $p(\mathcal{W}^{\perp})$ which represents our uncertainty in the unknown scale. Uncertainty specified in

the scale model is then incorporated into the conditional estimand as

$$\tilde{\theta} = \mathbb{E}_{p(\mathcal{W}^\perp)} f(\mathcal{W}^\perp, \mathcal{Y}) \quad (5)$$

which we term a *scale simulation estimator*.

5.1 Properties of Scale Simulation Estimators

We highlight key properties of scale simulation estimators, comparing and contrasting to current approaches and Bayesian PIMs.

Scale simulation estimators have at least two advantages over existing approaches. First, unlike current approaches which often use implicit identifying assumptions, the model building process explicitly uses the scale model of scale simulation. Scale models make it easy to identify potentially incorrect assumptions or to customize assumptions to better reflect a particular system under study. Second, scale simulation can account for uncertainty in assumptions regarding scale through a non-singular scale model.

Scale simulation estimators are intricately related to Bayesian PIMs. In fact, in Supplementary Section A.4, we prove that Bayesian PIMs are a special case of scale simulation estimators, where the scale model has a particular conditional relationship with the conditional estimand. We introduce scale simulation estimators to relax the need for this conditional relationship, so as to easily specify different scale models and use the same computationally efficient inference algorithms. While we demonstrate that scale simulation satisfies these requirements in the next subsection, here we show that this added flexibility does not sacrifice the core calibration properties of Bayesian PIMs.

Gustafson (2015) demonstrated that inference without identifiability necessitates a large sample bias: the bias introduced through the use of subjective assumptions remains even in the asymptotic limit. For Bayesian PIMs, the non-degeneracy of the prior encodes uncertainty in identifying assumptions, which also reflects an uncertainty in this large-

sample bias. These models have an asymptotic posterior variance that remains non-zero and calibrated with respect to the potential bias encoded in the prior (Gustafson, 2015). A proof of the following result is provided in Supplementary Section A.5.

Theorem 3. *Let $\tilde{f} = \mathbb{E}_{p(\mathcal{W}^\perp|\mathcal{W}^\parallel)} f(\mathcal{Y}^{(\rho,s)}, \mathcal{W}^\perp)$ be a scale simulation estimator with corresponding target estimand $f(\mathcal{W}^\parallel, \mathcal{W}^\perp)$ and measurement model $p(\mathcal{Y}^{(\rho,s)}|\mathcal{W}^\parallel)$ such that uncertainty in \mathcal{W}^\parallel tends to zero as $\rho \rightarrow \infty$ and $s \rightarrow \mathbf{M}$. Then the asymptotic variance of \tilde{f} is given by*

$$\lim_{\rho \rightarrow \infty, s \rightarrow \mathbf{M}} \text{Var}(\tilde{f} | \mathcal{Y}^{(\rho,s)}) \geq \int \left\{ \text{bias}(\tilde{f} | \mathcal{W}^{\parallel\dagger}, \mathcal{W}^\perp) \right\}^2 p(\mathcal{W}^\perp | \mathcal{W}^{\parallel\dagger}) d\mathcal{W}^\perp \quad (6)$$

where $\mathcal{W}^{\parallel\dagger}$ denotes the true value of \mathcal{W}^\parallel and with

$$\text{bias}(\tilde{f} | \mathcal{W}^{\parallel\dagger}, \mathcal{W}^\perp) = E_{p(\mathcal{W}^\perp | \mathcal{W}^{\parallel\dagger})} [f(\mathcal{W}^{\parallel\dagger}, \mathcal{W}^\perp)] - f(\mathcal{W}^{\parallel\dagger}, \mathcal{W}^\perp). \quad (7)$$

Compared to Bayesian PIMs (Gustafson, 2015, pgs. 35-36), scale simulation estimators have an identical asymptotic bias and identical lower bound variance to Bayesian PIMs. That is, the added flexibility of scale simulation estimators can lead to more conservative variance estimates. In Supplementary Section A.5, we show that if $f(\mathcal{W})$ is either a scalar estimand or a probabilistic estimand identified by \mathcal{W} , then this lower bound is achieved. In fact, not achieving this lower bound would imply that a target estimand was chosen that is not identifiable or unique even in the complete data setting. Based on these results, we argue that scale simulation estimators typically have the same efficiency as Bayesian PIMs.

This result also shows that uncertainty reflected in a scale model (i.e., $p(\mathcal{W}^\perp)$ or more generally $p(\mathcal{W}^\perp | \mathcal{W}^\parallel)$) is used as a model for potential large-sample bias. So long as the scale model is non-singular (i.e., not an identifying restriction), the estimator acknowledges its potential bias through a variance that remains non-singular even in the asymptotic limit. This result also explains the unacknowledged bias observed with DESeq2 and ALDEx2 in Figure 1. Both ALDEx2 and DESeq2 can be thought of as scale simulation estimators

that use a scale model that is an identifying restriction (e.g., data normalization). In Section 4.1, we provided an intuitive explanation for why this will be a biased estimator. Theorem 3 confirms that intuition: an identifying restrictions translates to an estimator whose asymptotic variance is singular or even zero despite a non-zero bias.

5.2 Simulation Estimators for Differential Analysis

We develop two scale simulation estimators for differential abundance analysis of sequence count data. We start by defining two distinct conditional estimands, one a generalization of the ALDEx2 model presented in Section 1.1, the other a generalization of Bayesian multinomial logistic-normal linear models. We then introduce a class of scale models that allow us to bridge the gap between current approaches to scale-reliant inference and the CoDA viewpoint of scale invariance.

5.2.1 An ALDEx2-based Conditional Estimand

We chose to generalize the ALDEx2 model for two reasons. First, to confirm that by considering uncertainty in identifying assumptions, we can mitigate or remove the unacknowledged bias we observed in Section 4.2. Second, to demonstrate how to adapt preferred models to fit within the scale simulation framework.

To represent ALDEx2 as a scale-simulation estimator, rewrite the ALDEx2 model as

$$Y_{\cdot j} \sim \text{Multinomial}(W_{\cdot j}^{\parallel}) \quad (8)$$

$$\eta_{\cdot j} = \log W_{\cdot j}^{\parallel} + \log W_{\cdot j}^{\perp} \quad (9)$$

$$W_{\cdot j}^{\parallel} \sim \text{Dirichlet}(\gamma) \quad (10)$$

where the posterior $p(\eta|Y, W^{\parallel})$ now represents a scale conditional estimand. Procedurally, for any scale model $p(W^{\perp})$, the expectation $\hat{\theta} = \mathbb{E}_{p(W^{\perp})} p(\eta|Y, W^{\parallel})$ can be evaluated using Monte Carlo integration: for each Monte Carlo sample, sample W^{\perp} from the scale model,

then sample W^{\parallel} from the Multinomial Dirichlet posteriors (which have no dependence on W^{\perp}), then calculate η using Equation (9).

5.2.2 A Multinomial Log-Normal Conditional Estimand

Bayesian multinomial logistic-normal models have become increasingly popular for the analysis of sequence count data (Silverman et al., 2018; Grantham et al., 2020). Following this literature suggests the following multinomial log-normal model could be appealing if the system scale were known:

$$\begin{aligned}\mathcal{Y}(j) &\sim \text{Multinomial}(\mathcal{W}(j)/\mathcal{W}(j)^{\perp}) \\ \mathcal{W}(j) &= e^{\psi_j} \\ \psi_j &\sim N(BX_j, \Omega)\end{aligned}$$

with priors $B \sim N(M, \Omega, V)$ and $\Omega \sim IW(u, \Xi)$. Since the system scale is not known, we consider the posterior $p(B, \Omega | \mathcal{Y}, \mathcal{W}^{\perp})$ to be a scale-conditional estimand. In Supplementary Section C, we show that this conditional estimand can be sampled with only a minor modification of the Collapse-Uncollapse sampler of Silverman et al. (2022).

Viewed as a conditional estimand, the posterior $p(B, \Omega | \mathcal{Y}, \mathcal{W}^{\perp})$ can be turned into a scale simulation estimator in at least two ways. The most direct is by taking the expectation of the posterior with respect to a scale model. In essence this approach simulates observations of \mathcal{W}^{\perp} from the scale model. If instead we treat \mathcal{W}^{\perp} as completely unobserved, the above model represents a Bayesian PIM. In fact, while we are unaware of any efficient means of directly sampling this PIM, in Section 6.2 and Supplementary Section C, we show how we can create a scale simulation estimator that is identical to the Bayesian PIM but can be inferred efficiently through direct Monte Carlo simulation.

5.2.3 A Log-Normal Family of Scale Models

Consider the family of scale models defined by:

$$\log f(\mathcal{W}(j)^\perp | \mu, \alpha) \sim N(c + \mu_j, \alpha^2)$$

for some constant c and with the constraint that $\sum_j \mu_j = 0$. This model describes the scale in each condition j using a log-normal distribution with mean parameter governed by a global scale c and a vector μ representing the relative scale in each condition. We decompose the mean into c and μ to ease model specification in the next section.

With this family, we develop a unified representation of the assumptions behind scale-invariant inference methods and the assumptions reflected in common identifying restrictions. Common identifying restrictions can be written as a degenerate point mass $p(\log \mathcal{W}^\perp) = \delta(\log \mathcal{W}^\perp = r)$ for some constant vector r . For example $r_j = -\log g(\mathcal{W}(j)^\parallel)$ for the CLR identifying restriction used by ALDEX2. These identifying restrictions can be represented in this log-normal scale model family by letting $(c + \mu) = r$ and considering the limit as $\alpha^2 \rightarrow 0$ (zero uncertainty). In contrast, the requirement for scale-invariance equates to the opposite extreme: an assumption of infinite uncertainty in the system scale which can be represented as the special case where $\alpha \rightarrow \infty$. Of course this family will also let us specify scale models between these two extremes.

5.3 Sensitivity Analysis through Scale Simulation

To guarantee the properties discussed in Section 5.1, we must consider requirements on the choice of scale model. There are two ways of framing the requirement on scale models. From the perspective of subjective probability, estimator calibration is predicated on the assumption that the scale model faithfully represents the researcher's beliefs. From an objective inference perspective, estimator calibration requires that the scale model accurately models the estimator's bias. From either viewpoint, we expect that the challenge of model

specification will violate these assumptions in practice. To address this limitation, we introduce a type of sensitivity analysis that can allow analysts to investigate the sensitivity of results to their chosen scale model.

Both the partially identified models and causal inference literature have proposed sensitivity analysis to address unidentifiability from unmeasured confounding in observational studies (Rosenbaum and Rubin, 1983; Greenland, 2005). In those fields, an analysis is repeated over a range of possible values for the unmeasured confounder. Intuitively, if a conclusion drawn from the data is insensitive to the value of the unmeasured confounder, then the conclusion is unlikely to be spurious secondary to the confounding factor.

Here, we slightly modify this approach. Whereas confounding factors in observational studies are often low-dimensional, the scale of a system grows linearly with the number of conditions in a study. So it is often infeasible to interpret a sensitivity analysis performed over the full set of possible scales \mathcal{W}^\perp . Thus we propose performing sensitivity analysis with respect to a small number of parameters in a family of scale models defined over this set. We term this *scale sensitivity analysis*.

While global sensitivity analyses are often impractical in Bayesian inference due to computational expense, we can often exploit the structure of scale simulation estimators for efficient global sensitivity analyses. In general, the expectation in Equation (5) will be approximated using Monte Carlo integration, which requires paired samples of \mathcal{W}^\perp and \mathcal{W}^\parallel for a given target estimand. For most problems, the former will be far less computationally intensive than the latter, due to the higher dimension of \mathcal{W}^\parallel and the dependence of \mathcal{W}^\parallel on real data. But we expect that for many conditional estimands, inference of \mathcal{W}^\parallel will be independent of \mathcal{W}^\perp , so each evaluated scale model can store and reuse samples of \mathcal{W}^\parallel . For example, for the ALDEx2-based conditional estimand introduced above, sampling \mathcal{W}^\parallel is independent of \mathcal{W}^\perp , allowing samples of \mathcal{W}^\parallel to be reused between scale models. In Supplementary Section C, we demonstrate that a similar independence holds for the Bayesian

multinomial log-normal conditional estimands and provide an algorithm for exploiting this independence for scale simulation analyses.

6 Real and Simulated Data Analysis

6.1 Simulated Data Analysis

In Section 4, our simulation demonstrated that ALDEx2 (and DESeq2) suffered from an unacknowledged bias which led to increasing Type-I error with increasing sample size. Here, we mitigate this unacknowledged bias by accounting for uncertainty in identifying assumptions in our simulated example.

Recall that the simulation in Section 4 consisted of 21 bacterial taxa, 4 of which truly decrease in abundance after a mild antibiotic treatment. Here, we simulate 100 measurements, 50 replicates from the pre-antibiotic condition and 50 replicates from the post-antibiotic condition. We compare 6 models: DESeq2, ALDEx2, and 4 scale simulation estimators built from the ALDEx2-based conditional estimand paired with different log-normal scale models. The first scale model, which we term the CLR scale model, represents the CLR identifying restriction and is given by $\alpha \rightarrow 0$, and $(c + \mu) = r$ for $r_j = -\log(g(\mathcal{W}(j)^\parallel))$. The second represents the uncertainty of CoDA’s axiom of scale invariance and is given by $\alpha \rightarrow \infty$. The third and fourth scale models, described next, represent a middle-ground between these two extremes.

In a real study of human microbiota, we would have little prior knowledge regarding the global scale of the system c , and would appeal to basic biological plausibility to choose the parameters μ and α . For example, since this is a mild antibiotic, we expect the scale between conditions is similar: we believe it is implausible that the scale between conditions would change by more than a factor of 1.5 and that the scale within conditions would rarely vary by more than a factor of 3. Staying with the log-normal scale model family, we can encapsulate

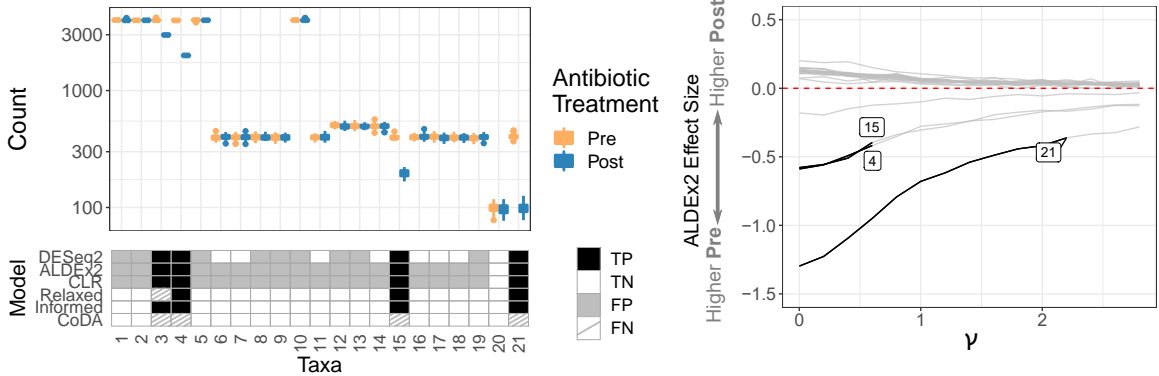


Figure 2: (Top Left) True simulated abundances of 21 taxa between two conditions. Four of 21 taxa were truly differentially abundant between conditions, all decreasing post-treatment. To simulate the loss of scale information, the total number of counts for each sample was subsampled to 5,000 prior to modeling. Further simulation details can be found in Supplementary Section B. (Bottom Left) Final discovery of each taxa by method. (Right) Sensitivity analysis showing the estimated ALDEx2 effect size (see Supplementary Section B) for each taxa under the Relaxed model as a function of γ with $\alpha = 0.60$. A black line signifies that the estimated effect size was statistically different from zero with 95% certainty. These results show that even small relaxations from infinitesimal identifying restrictions can greatly improve inference over traditional methods.

this belief by expressing the location parameter μ_j as a function of the antibiotic treatment status, i.e., $\mu_j = \beta X_j$ where $\beta \sim N(0, \gamma^2)$ and X_j denotes the treatment status of sample j , and scale parameters $\alpha = 0.6$ and $\gamma = 0.2$. We call this the *relaxed* model. We also consider a situation in which we have external identifying measurements, e.g., some technology that provides a potentially noisy, yet unbiased, measurement of the scale. We denote these measurements as z_j and specify $\mu_j = z_j$ and $\alpha = 0.5$ where we assume a measurement standard error of 0.5. We call this the *informed* model. All code required to reproduce our analysis can be found at <https://github.com/michellepistner/scaleSimulation>.

The results are shown in Figure 2 (left panels). Unsurprisingly, the CoDA estimator led to fully scale invariant results: the model concluded that no conclusions about differential abundance were possible (always accepting the null). At the other extreme, ALDEx2 and

the CLR estimator produced identical results (and nearly identical to DESeq2). All three of these methods demonstrated high false discovery rates. Remarkably, the DESeq2 estimator imputes the system scale highly accurately, but produces this high false discovery rate due to over-certainty in its imputed estimates (i.e., low bias but even lower variance; see Supplementary Section D.2 for details). By relaxing the CLR estimator and incorporating uncertainty in the scale model, the Relaxed estimator gave no false positives at the expense of only a single false negative. Moreover, Supplemental Figure 1 shows that the relaxed estimator avoids the unacknowledged bias seen with DESeq2 and ALDEx2 in Figure 1. Finally, and not unexpectedly, the Informed estimator achieves perfect performance. Together, these results demonstrate the ease with which scale simulation can be implemented and the importance of accounting for uncertainty in identifying assumptions. Scale simulation can provide a unified conceptual foundation on which both scale reliant and scale invariant methods can be represented, generalized, and evaluated.

It is unclear if the performance of the Relaxed model would change substantially with a different values of α or γ . To address this concern, we used scale sensitivity analysis to investigate how the inferred differential abundance of each taxa in the study varies with the choice of the parameter γ (Figure 2, right panel) and α (Supplementary Figure 1, left panel). Together these figures show that, out uncertainty encoded in either the parameter $\alpha = 0.6$ or $\gamma = 0.2$ alone is too great to draw any conclusions about taxa 3. In contrast, this figure also shows that our conclusions regarding taxa 4, 15, and 21 are unlikely to be spurious secondary to our chosen scale model. This figure shows that our conclusions in regards to these three taxa hold so long as we believe (with $\geq 95\%$ certainty) that the true differences in scales between conditions is less than a factor of 2.5 (e.g., $e^{1.96 \times 0.5}$).

6.2 Real Data Analysis

To investigate unacknowledged bias and demonstrate scale simulation with real data, we analyzed a novel study which aimed to capture how bioreactors (*ex vivo* artificial gut systems) deviate from the host-derived microbial communities used to inoculate them. Specifically, the study aimed to identify which microbial taxa increased or decreased in abundance between day 1 (immediately after inoculation) and day 14 (after the “burn-in period”, Silverman et al. (2018)). Twelve conditions were studied: 6 bioreactors, each sampled at the two time-points. 16S rRNA measurements were taken in each vessel from each day; flow cytometry measurements were used to measure total microbial concentration following methods outlined in Vandeputte et al. (2017). As the bioreactors were kept at a fixed volume, concentration was proportional to the true total microbial abundance. Measurements were taken 2-3 times for each condition to capture the technical error in flow cytometry.

Based on our prior work analyzing artificial gut studies (Silverman et al., 2018), we chose our scale conditional estimand as the Bayesian multinomial log-normal linear conditional estimand presented in Section 5.2.2. As covariates X_j , we included a random intercept for each of the 6 vessels and a binary variable representing the two time-points. For our prior parameters, we set: $\nu = D + 3$ and $\Xi = I_D$ reflecting our weak prior knowledge that the taxa were independent; $\Gamma = \text{BlockDiagonal}(10I_6, 1)$ reflecting our assumption that the some taxa were more abundant than others at baseline and assuming that the signal-to-noise ratio with respect to differential abundance was most likely on the order of 1 (Silverman et al., 2018); and finally $M = 0$ which reflected that we did not have *a priori* knowledge differentiating the taxa.

Given the design of this experiment, the total abundance of bacteria in each condition was identifiable from flow cytometry measurements. Moreover, the presence of technical replicates allowed us to estimate the scale model directly from the flow cytometry mea-

surements:

$$\log f(W_j^\perp) \sim N(\mu_j, \sigma_j^2)$$

where μ_j and σ_j^2 denote the mean and variance of the log-transformed flow cytometry measurements from condition j . We call the estimator formed from combining this scale model with the above multinomial log-normal estimand the *flow* estimator. Setting this estimator as our gold standard, we evaluated the performance of other methods. Beyond ALDEx2 and DESeq2, we also created a scale simulation estimator that did not have access to these flow cytometry measurements and reflected our prior beliefs based on the design of the experiment. We call this the *design-based* estimator.

The design-based estimator is a straightforward extension of our previous scale model. In this study, each vessel contained 400 mL of microbial growth media and was inoculated with 100 mL of fecal slurry. We expected that the total microbial load would increase from the day 1 to day 14 time-point by a factor of approximately 4. We encapsulated these beliefs in the scale model:

$$\frac{f(W_{j,t=1}^\perp)}{f(W_{j,t=14}^\perp)} \sim \text{LogNormal}(\bar{d}, \tau^2)$$

where $\bar{d} = \log(100/400)$ and $\tau = 1$.⁴ We call this the *design-based scale model*. All code required to reproduce our analysis can be found at <https://github.com/michellepistner/scaleSimulation>.

Using the flow estimator, we found evidence that 9 taxa differentially increased and 2 differentially decreased with probability $\geq 95\%$. In contrast to our simulation study in Section 5.2.1, the scales between conditions change substantially: $\mathbb{E} \log[W_{(t=1)}^\perp / W_{(t=14)}^\perp] = -1.22$. In this setting, ALDEx2 and DESeq2 display reasonable specificities (96.8% and 100%, respectively) and false discovery rate (20% and 0%, respectively) but poor sensitivity (40% and 50%, respectively). In contrast, the design-based estimator achieves a specificity of 100%, a false discovery rate of 0%, and a sensitivity of 90% despite a similar degree of

⁴ τ^2 can be compared to σ^2 in the flow estimator by the relationship $\tau^2 = 2\sigma^2$.

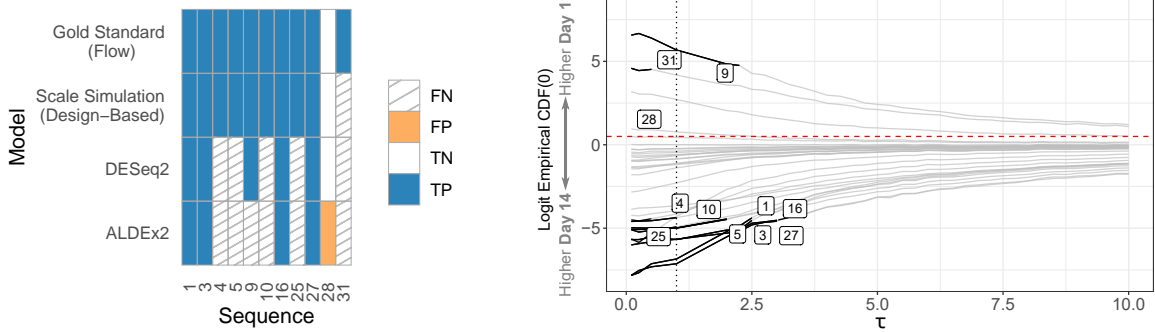


Figure 3: (Left) Comparison of output across selected models. The top row denotes the Gold Standard (Flow) model which we use as truth when comparing the various other models. (Right) A scale sensitivity analysis showing how results in the design-based model change as a function of α versus the Logit-transformed Empirical CDF evaluated at zero. This measure captures the model's certainty in differential abundance. Small and large values indicate differential increases and decreases, respectively. Values near 0 indicate the posterior distribution is evenly distributed between positive and negative differential abundance. The taxonomic identity of each sequence is provided in Supplementary Table 1.

misspecification as the ALDEx2 and DESeq2 models ($\bar{d} = -3.0$). Finally, in Supplementary Section D.1, we use bootstrap resampling to show that a dataset with more replicates would have led to a higher false positive rate stemming from an unacknowledged bias. With 50 vessels, DESeq2 and ALDEx2 give FDRs of 39.3% and 45.16%, respectively. In contrast, the design-based model remains calibrated with an FDR of 0.00%. Together, these results again demonstrate the utility of accounting for uncertainty in identifying assumptions and the value of making these assumptions an explicit part of the model building process.

Finally, to demonstrate how scale simulation can provide an efficient means of inferring Bayesian PIMs, we demonstrate in Supplementary Section D.3 that the above multinomial log-normal model can be inferred as a Bayesian PIM using scale simulation. The Bayesian PIM demonstrated a sensitivity of 80% and specificity of 96.8%.

7 Discussion

We have introduced new theory and tools for studying compositional surveys. We have demonstrated that many common analyses performed on compositional surveys are fully scale reliant and cannot satisfy standard criteria required for Frequentist inference. Contrary to the CoDA viewpoint, we find that principled inference is possible if we move to a Bayesian perspective or accept the weaker Bayesian notion of interval calibration. Regardless of the chosen approach, our results highlight the importance of considering uncertainty or error in the assumptions used to identify inference. To aid in such analyses, we have proposed scale simulation estimators and scale sensitivity analysis, which we believe will find broad utility in the analysis of compositional surveys.

We note three areas of potentially fruitful future work. First, though we introduced scale simulation through its connections to Bayesian PIMs, we believe it could also be introduced from the perspective of causal inference or methods for addressing missing data. Scale conditional estimands resemble causal estimands and scale models resemble either missing data mechanisms in the analysis missing data or assignment mechanisms in causal inference. Second, in the specific application of sequence count data analysis, other key data limitations can cause models to be unidentifiable. These include standard limitations such as improper study design and inadequate sample size, or more specialized limitations such as measurement bias. As with limitations that arise from the lack of scale information, we suggest that careful consideration of uncertainty introduced due to those data limitations may be key to overcoming those challenges. Third, we have focused our examples on differential abundance in microbiome systems, but scale reliant inference goes beyond both microbiome systems and differential analysis. Overall, there are many areas for future work.

Acknowledgments and Funding Sources

We thank Rachel Silverman, Juan Jose Egozcue, Vera Pawlosky-Glahn, Gregory Gloor, Michael Love, and James Morton for their manuscript comments. LAD acknowledges support from the the Global Probiotics Council, a Searle Scholars Award, the Hartwell Foundation, an Alfred P. Sloan Research Fellowship, the Translational Research Institute through Cooperative Agreement NNX16AO69A, the Damon Runyon Cancer Research Foundation, and NIH 1R01DK116187-01. SM would like to acknowledge the support of grants NSF IIS-1546331, NSF DMS-1418261, NSF IIS-1320357, NSF DMS-1045153, and NSF DMS-1613261.

References

Aitchison, J. (1982). The statistical analysis of compositional data. *Journal of the Royal Statistical Society: Series B (Methodological)*, 44(2):139–160.

Chiquet, J., Mariadassou, M., and Robin, S. (2021). The poisson-lognormal model as a versatile framework for the joint analysis of species abundances. *Frontiers in Ecology and Evolution*, 9:188.

Choi, Y., Coram, M., Peng, J., and Tang, H. (2017). A poisson log-normal model for constructing gene covariation network using RNA-seq data. *Journal of Computational Biology*, 24(7):721–731.

Fang, H., Huang, C., Zhao, H., and Deng, M. (2015). CCLasso: correlation inference for compositional data through lasso. *Bioinformatics*, 31(19):3172–3180.

Fernandes, A. D., Reid, J. N., Macklaim, J. M., McMurrough, T. A., Edgell, D. R., and Gloor, G. B. (2014). Unifying the analysis of high-throughput sequencing datasets:

characterizing RNA-seq, 16S rRNA gene sequencing and selective growth experiments by compositional data analysis. *Microbiome*, 2(1):1–13.

Friedman, J. and Alm, E. J. (2012). Inferring correlation networks from genomic survey data. *PLoS Computational Biology*, 8(9):e1002687.

Grantham, N. S., Guan, Y., Reich, B. J., Borer, E. T., and Gross, K. (2020). Mimix: A bayesian mixed-effects model for microbiome data from designed experiments. *Journal of the American Statistical Association*, 115(530):599–609.

Greenland, S. (2005). Multiple-bias modelling for analysis of observational data. *Journal of the Royal Statistical Society: Series A (Statistics in Society)*, 168(2):267–306.

Gustafson, P. (2015). *Bayesian inference for partially identified models: Exploring the limits of limited data*, volume 140. CRC Press.

Hawinkel, S., Mattiello, F., Bijnens, L., and Thas, O. (2019). A broken promise: microbiome differential abundance methods do not control the false discovery rate. *Briefings in Bioinformatics*, 20(1):210–221.

Imbens, G. W. and Manski, C. F. (2004). Confidence intervals for partially identified parameters. *Econometrica*, 72(6):1845–1857.

Jarauta Bragulat, E., Egozcue, J. J., et al. (2011). Approaching predator-prey lotka-volterra equations by simplicial linear differential equations. 4th International Workshop on Compositional Data Analysis.

Jeganathan, P. and Holmes, S. P. (2021). A statistical perspective on the challenges in molecular microbial biology. *Journal of Agricultural, Biological and Environmental Statistics*, 26(2):131–160.

Kurtz, Z. D., Müller, C. L., Miraldi, E. R., Littman, D. R., Blaser, M. J., and Bonneau, R. A. (2015). Sparse and compositionally robust inference of microbial ecological networks. *PLoS Computational Biology*, 11(5):e1004226.

Love, M. I. (2021). *Statistical Modeling of High Dimensional Counts*. Springer.

Love, M. I., Huber, W., and Anders, S. (2014). Moderated estimation of fold change and dispersion for RNA-seq data with DESeq2. *Genome Biology*, 15(12):1–21.

Lovell, D., Pawlowsky-Glahn, V., Egozcue, J. J., Marguerat, S., and Bähler, J. (2015). Proportionality: a valid alternative to correlation for relative data. *PLoS Computational Biology*, 11(3):e1004075.

Martín-Fernández, J., Egozcue, J. J., Olea, R., and Pawlowsky-Glahn, V. (2021). Units recovery methods in compositional data analysis. *Natural Resources Research*, 30(4):3045–3058.

McMurdie, P. J. and Holmes, S. (2014). Waste not, want not: why rarefying microbiome data is inadmissible. *PLoS Computational Biology*, 10(4):e1003531.

Morton, J. T., Marotz, C., Washburne, A., Silverman, J., Zaramela, L. S., Edlund, A., Zengler, K., and Knight, R. (2019). Establishing microbial composition measurement standards with reference frames. *Nature Communications*, 10(1):1–11.

Neath, A. A. and Samaniego, F. J. (1997). On the efficacy of bayesian inference for non-identifiable models. *The American Statistician*, 51(3):225–232.

Pawlowsky-Glahn, V., Egozcue, J. J., and Lovell, D. (2015a). Tools for compositional data with a total. *Statistical Modelling*, 15(2):175–190.

Pawlowsky-Glahn, V., Egozcue, J. J., and Tolosana-Delgado, R. (2015b). *Modeling and analysis of compositional data*. John Wiley & Sons.

Pendegraft, A. H., Guo, B., and Yi, N. (2019). Bayesian hierarchical negative binomial models for multivariable analyses with applications to human microbiome count data. *PloS One*, 14(8):e0220961.

Quinn, T. P., Erb, I., Richardson, M. F., and Crowley, T. M. (2018). Understanding sequencing data as compositions: an outlook and review. *Bioinformatics*, 34(16):2870–2878.

Rosenbaum, P. R. and Rubin, D. B. (1983). Assessing sensitivity to an unobserved binary covariate in an observational study with binary outcome. *Journal of the Royal Statistical Society: Series B (Methodological)*, 45(2):212–218.

Schwager, E., Mallick, H., Ventz, S., and Huttenhower, C. (2017). A bayesian method for detecting pairwise associations in compositional data. *PLoS Computational Biology*, 13(11):e1005852.

Silverman, J. D., Durand, H. K., Bloom, R. J., Mukherjee, S., and David, L. A. (2018). Dynamic linear models guide design and analysis of microbiota studies within artificial human guts. *Microbiome*, 6(1):1–20.

Silverman, J. D., Roche, K., Holmes, Z. C., David, L. A., and Mukherjee, S. (2022). Bayesian multinomial logistic normal models through marginally latent matrix-t processes. *Journal of Machine Learning Research*, 23(7):1–42.

Srinivasan, A., Xue, L., and Zhan, X. (2020). Compositional knockoff filter for high-dimensional regression analysis of microbiome data. *Biometrics*.

Vandeputte, D., Kathagen, G., D’hoe, K., Vieira-Silva, S., Valles-Colomer, M., Sabino, J., Wang, J., Tito, R. Y., De Commer, L., Darzi, Y., et al. (2017). Quantitative microbiome profiling links gut community variation to microbial load. *Nature*, 551(7681):507–511.

Verma, D., Garg, P. K., and Dubey, A. K. (2018). Insights into the human oral microbiome. *Archives of Microbiology*, 200(4):525–540.

Supplement to “A Statistical Analysis of Compositional Surveys”

Michelle Pistner Nixon, Jeffrey Letourneau, Lawrence A. David,
Sayan Mukherjee, and Justin D. Silverman

In this supplement, we present the proofs to our main results and additional claims made throughout the paper. In addition, we show additional details and results of our simulations and data analyses.

A Definitions and Proofs of Results

This section contains the proofs for each of the results in the main text and formal definitions of necessary terms.

A.1 Proofs of Proposition 1 and Theorems 1 and 2

Lemma A.1. *Let \mathcal{Y} denote a fully compositional survey of a scaled system \mathcal{W} . If the target model $P_\theta(\mathcal{W})$ is scale reliant, then θ is partially or fully unidentified by \mathcal{Y} . If the target model is fully scale reliant, then θ is fully unidentified by \mathcal{Y} .*

Proof. Starting with the fully scale reliant case. By contradiction, suppose that the parameter θ is not fully unidentified by a compositional survey, i.e., $\text{Id}_\theta(Y) \subset \Theta$. We also have that $\text{Id}_\Theta(\mathcal{W}^\parallel) = \Theta$, and $\text{Id}_{\mathcal{W}^\perp}(\mathcal{Y}) = \mathbf{W}^\perp$ where \mathbf{W}^\perp denotes the set of all possible system scales. Then there must be some $\theta^* \in \Theta$ such that $\theta^* \notin \text{Id}_\theta(\mathcal{Y})$. Since $\text{Id}_\Theta(\mathcal{W}^\parallel) = \Theta$ this implies that the compositional survey must have provided some restriction on the set of all possible scales which contradicts $\text{Id}_{\mathcal{W}^\perp}(\mathcal{Y}) = \mathbf{W}^\perp$.

Next for the partially scale reliant case. By contradiction, suppose that the parameter θ is identified by a fully compositional survey, i.e., $\text{Id}_\theta(Y)$ is a singleton set. We also have that $\text{Id}_\Theta(\mathcal{W}^\parallel) \subset \Theta$, and $\text{Id}_{\mathcal{W}^\perp}(\mathcal{Y}) = \mathbf{W}^\perp$

where \mathbf{W}^\perp denotes the set of all possible system scales. Then there must be only one $\theta^* \in \Theta$ satisfying $\theta^* \notin \text{Id}_\theta(\mathcal{Y})$. Since $\text{Id}_\Theta(\mathcal{W}^\parallel) \subset \Theta$ and $\text{Id}_\Theta(\mathcal{W}^\parallel)$ is not a singleton set this implies that the compositional survey must have provided some restriction on the set of all possible scales which contradicts $\text{Id}_{\mathcal{W}^\perp}(\mathcal{Y}) = \mathbf{W}^\perp$. \square

Our proof of the following theorem is patterned off of Gabrielsen (1978).

Theorem 1. *Let \mathcal{Y} denote a fully compositional survey or a partially compositional survey under the noisy data assumption. If $\theta \in \Theta$ is a scale reliant parameter, then there does not exist a sequence of estimators $\{\hat{\theta}^{(\rho,s)}\}$ based on \mathcal{Y} that is consistent.*

Proof. By contradiction, suppose that θ is a scale reliant parameter and that there exists a min- ρ sequence of estimators $\{\hat{\theta}_S(\mathcal{Y}^{(\rho)})\}$ that is consistent. Since θ is a scale reliant parameter, it follows from Lemma A.1 that θ is unidentifiable given a compositional survey \mathcal{Y} of \mathcal{W} . Since θ is unidentifiable, then there exist at least two distinct values $\theta_i, \theta_j \in \Theta$ that yield the exact same distribution of $\mathcal{Y}^{(\rho)}$. Since $\hat{\theta}^{(\rho,s)}$ is a consistent sequence of estimators then it must converge to both θ_i and θ_j which is a contradiction. \square

Theorem 2. *If $\theta \in \Theta$ is fully unidentifiable given a random variable X , then there does not exist a usable confidence set of the form $S(X)$.*

Proof. By contradiction, suppose $S(X)$ is a usable confidence set for a parameter $\theta \in \Theta$ that is fully unidentifiable given X . Since $S(X)$ is a usable confidence set, then for any $\theta_i \in \Theta$, there must be some other $\theta_j \in \Theta$ such that $P_{\theta_i}(\theta_j \notin S(X)) = 1$. However, by Definition 2, since θ is fully unidentifiable given X , every two $\theta_i, \theta_j \in \Theta$ can yield the exact same distribution of X . Therefore, if $\beta > 0$, both θ_i and θ_j must be in the set $S(X)$. This is a contradiction. \square

A.2 Partially Compositional Surveys

Here we provide an extended discussion of partially compositional surveys and motivate our focus on fully compositional surveys (or partially compositional surveys under the noisy data assumption) in the main text.

Following the main text, we note that there are additional criteria that must be satisfied for a fully scale reliant parameter to be only partially unidentifiable or identifiable. If \mathcal{Y} is a partially compositional survey, then

$\text{Id}_{\mathcal{W}^\perp}(\mathcal{Y}) \subset \mathbf{W}^\perp$. Let $\bar{\mathbf{W}}^\perp$ denote the complement of this set. Clearly, the compositional survey allows us to exclude the set $\bar{\mathbf{W}}^\perp$ from consideration. Also, by the definition of a compositional survey, $\text{Id}_{\mathcal{W}^\parallel}(Y)$ is a singleton set. It is not difficult to see that the partially compositional survey provides information about both the composition and the scale of \mathcal{W} . However, translating this to a statement about the identifiability of θ requires further discussion. If, for example, the parameter of interest is differential abundance $\theta_i = \mathbb{E} \log(\mathcal{W}_{i(x=1)}^\parallel / \mathcal{W}_{i(x=0)}^\parallel)$, and the information provided by \mathcal{Y} relates only to the sum of the system scale $\sum_m \mathcal{W}(m)^\perp$ (i.e., $\bar{\mathbf{W}}^\perp$ is the equivalence class formed from all $\mathcal{W}^\perp \in \mathbf{W}^\perp$ such that for all $c \in \mathbb{R}^+$ \mathcal{W}^\perp satisfies $\mathcal{W}(m)^\perp = c\mathcal{W}(m)^\perp \forall m, \sum_m \mathcal{W}(m)^\perp = 1$), then θ_i is still fully unidentified by the compositional survey. Moreover, even if the compositional survey provides non-trivial information about the system scale, the value of this information is directly tied to the size of the identification region: if \mathbf{W}^\perp is large, then it may not overcome the uncertainty introduced by sampling noise (e.g., the noisy data assumption). Of note, we are unaware of any non-trivial situation in which a fully scale reliant parameter would be identified by a partially compositional survey although we know that it is theoretically possible.

This discussion also motivates our focus on the fully compositional survey regime. To further motivate this choice, we note that a major focus of this work is proving that, contrary to the scale invariance axiom of CoDA, principled scale reliant inference is possible. If we can show it is possible in the fully compositional survey regime, then it follows that it will hold in the partially compositional survey regime.

A.3 SparCC Imposes an Infinitesimal Identifying Restriction

Covariation in the scaled abundance between taxa or genes is often of scientific interest, i.e., estimates of the covariance between log scaled abundances:

$$\Sigma_{ij} = \text{cov}(\log(\mathcal{W}_i), \log(\mathcal{W}_j)).$$

Proposition A.1. *Consider a model $p(\mathcal{W}|\Sigma)$ parameterized by the covariance between dimensions of \mathcal{W} , i.e.,*

$$\Sigma_{ij} = \text{cov}(\log(\mathcal{W}_i), \log(\mathcal{W}_j)).$$

Each Σ_{ij} is a fully scale-reliant parameter.

Proof. We may reparameterize each Σ_{ij} in terms of $(\mathcal{W}^{\parallel}, \mathcal{W}^{\perp})$:

$$\begin{aligned}\Sigma_{ij} &= \text{cov}(\log \mathcal{W}_i^{\parallel} + \log \mathcal{W}_j^{\perp}, \log \mathcal{W}_j^{\parallel} + \log \mathcal{W}_i^{\perp}) \\ &= \text{cov}(\log \mathcal{W}_i^{\parallel}, \log \mathcal{W}_j^{\parallel}) + \text{cov}(\log \mathcal{W}_i^{\parallel}, \log \mathcal{W}_i^{\perp}) \\ &\quad + \text{cov}(\log \mathcal{W}_j^{\perp}, \log \mathcal{W}_j^{\parallel}) + \text{cov}(\log \mathcal{W}_j^{\perp}, \log \mathcal{W}_i^{\perp})\end{aligned}$$

Without loss of generality, given any \mathcal{W}^{\parallel} we can always specify \mathcal{W}^{\perp} such that $\text{cov}(\log \mathcal{W}_i^{\perp}, \log \mathcal{W}_j^{\parallel}) = 0$ leading to

$$\Sigma_{ij} = \text{cov}(\log \mathcal{W}_i^{\parallel}, \log \mathcal{W}_j^{\parallel}) + \text{var}(\log \mathcal{W}_i^{\perp}, \log \mathcal{W}_j^{\perp}).$$

It follows that given any \mathcal{W}^{\parallel} , for any two distinct $\Sigma_{ij}^{(1)}$ and $\Sigma_{ij}^{(2)}$, there exist two $\mathcal{W}^{\perp(1)}$ and $\mathcal{W}^{\perp(2)}$ such that $p(\mathcal{W}^{(i)\perp}, \mathcal{W}^{\parallel} | \theta^{(i)}) = p(\mathcal{W}^{\perp(j)}, \mathcal{W}^{\parallel} | \theta^{(j)})$. \square

To avoid this limitation, several methods have been proposed to infer dependence based on the relative abundances. Introduced by Friedman and Alm (2012), SparCC is a technique to characterize the dependencies between taxa of interest. Formally, SparCC estimates the covariance between the relative abundance of two taxa, i.e.:

$$\begin{aligned}\Omega_{ij} &= \text{cov}(\log(\mathcal{W}_i^{\parallel}), \log(\mathcal{W}_j^{\parallel})) \\ &= \text{var}(\log(\mathcal{W}_i^{\parallel}) - \log(\mathcal{W}_j^{\parallel})) \\ &= \omega_i^2 - \omega_j^2 - 2r_{ij}\omega_i\omega_j,\end{aligned}$$

where r_{ij} denotes the correlation between the relative abundances of taxa i and j . However, this system of equations is underdetermined: for D taxa, there are $D(D - 1)/2$ equations and $D(D + 1)/2$ unknowns (Friedman and Alm, 2012). To circumvent this, SparCC introduces a sparsity assumption which can be represented as

$$\Omega_{ij} \approx (D - 1)\omega_i^2 + \sum_{j \neq i} \omega_j^2. \tag{1}$$

See Friedman and Alm (2012) for full derivation.

Proposition A.2. *The sparsity assumption imposed by SparCC in Equation 1 is an example of an infinitesimal identifying restriction for estimating dependence between taxa, i.e:*

$$\Omega_{ij} = \text{cov}(\log(\mathcal{W}_i^{\parallel}), \log(\mathcal{W}_j^{\parallel})).$$

Proof. Recall that SparCC measures the covariance between the relative abundance of two taxa. These relative abundances can be re-parameterized in terms of the absolute abundances and the unknown scale of the system:

$$\begin{aligned} \text{cov}(\log(\mathcal{W}_i^{\parallel}), \log(\mathcal{W}_j^{\parallel})) &= \text{cov}(\log(\mathcal{W}_i) - \log(\mathcal{W}_i^{\perp}), \log(\mathcal{W}_j) - \log(\mathcal{W}_j^{\perp})) \\ &= \text{cov}(\log(\mathcal{W}_i^{\parallel}), \log(\mathcal{W}_j^{\parallel})) - \text{cov}(\log(\mathcal{W}_i^{\parallel}), \log(\mathcal{W}_j^{\perp})) \\ &\quad - \text{cov}(\log(\mathcal{W}_i^{\perp}), \log(\mathcal{W}_j^{\parallel})) + \text{cov}(\log(\mathcal{W}_i^{\perp}), \log(\mathcal{W}_j^{\perp})). \end{aligned}$$

Since there are more unknowns than equations, this system is underdetermined, and an infinite number of solutions exist. Again letting $\omega_i^2 = \text{var}(\log(\mathcal{W}_i^{\parallel}))$, we can rewrite the sparsity assumption of SparCC (Equation 1) as a system of equations:

$$Q\tilde{\omega} = \Omega,$$

where Q is a $P \times P$ matrix with d on the diagonal and 1 on the off diagonal and $\tilde{\omega} = [\omega_1^2, \dots, \omega_D^2]$. Since Q and $Q|\Omega$ have full and equal ranks, there is a unique solution for $\tilde{\omega}$. This implies that the estimated solution from SparCC is unique. \square

A.4 Scale Simulation as a Generalization of Bayesian PIMs

Theorem A.2 (Scale Simulation is a Generalization of Bayesian PIMs). *For a compositional survey \mathcal{Y} of a scaled system \mathcal{W} , any Bayesian PIM with a posterior of the form $p(\theta|\mathcal{Y})$ is expressible as a scale simulation estimator.*

Proof.

$$p(\theta|\mathcal{Y}) = \int p(\theta|\mathcal{W})p(\mathcal{W}|\mathcal{Y})d\mathcal{W}$$

From Definition 4 this is equivalent to

$$\begin{aligned} p(\theta|\mathcal{Y}) &= \int p(\theta|\mathcal{W}^{\parallel}, \mathcal{W}^{\perp})p(\mathcal{W}^{\parallel}|\mathcal{Y})p(\mathcal{W}^{\perp}|\mathcal{W}^{\parallel})d\mathcal{W} \\ &= E_{p(\mathcal{W}^{\perp}|\mathcal{W}^{\parallel})} [p(\theta|\mathcal{W}^{\parallel}, \mathcal{W}^{\perp})p(\mathcal{W}^{\parallel}|\mathcal{Y})]. \end{aligned}$$

It is therefore clear that that $p(\theta|\mathcal{Y})$ is a scale simulation estimator, with a scale conditional estimand of $p(\theta|\mathcal{W}^{\parallel}, \mathcal{W}^{\perp})p(\mathcal{W}^{\parallel}|\mathcal{Y})$ and a scale model of $p(\mathcal{W}^{\perp}|\mathcal{W}^{\parallel})$. \square

A.5 Misspecification of Scale Model Leads to Acknowledged Bias

The following notation, theorems, and proofs follow similar results given by Gustafson (2015, pages 24-36) with regards to Bayesian PIMs.

Notation: Let $\{\mathcal{Y}^{(\rho,s)}\}$ denote a min- ρ sequence of compositional surveys over $s \in \mathbf{M}$ conditions. Let the superscript \dagger denote the true value of a parameter or random variable, e.g., $\mathcal{W}(m)^{\parallel\dagger}$ denotes the true value of the composition of a scaled system in condition m . Finally, let $g(\mathcal{W}^{\parallel})$ denote expectation of the target estimand with respect to a chosen scale model, i.e.,

$$\begin{aligned} g(\mathcal{W}^{\parallel}) &= \mathbb{E}[f(\mathcal{W}) | \mathcal{W}^{\parallel}] \\ &= \int f(\mathcal{W}^{\parallel}, \mathcal{W}^{\perp}) p(\mathcal{W}^{\perp} | \mathcal{W}^{\parallel}) d\mathcal{W}^{\perp}. \end{aligned}$$

Theorem A.3. Let $\tilde{\theta} = \mathbb{E}_{p(\mathcal{W}^{\perp})} f(\mathcal{Y}^{(\rho,s)}, \mathcal{W}^{\perp})$ be a scale simulation estimator with target estimand $f(\mathcal{W}^{\parallel}, \mathcal{W}^{\perp}) = f(\mathcal{W})$. The large sample bias of $\tilde{\theta}$, i.e.,

$$bias(\tilde{\theta} | \mathcal{W}^{\parallel\dagger}, \mathcal{W}^{\perp\dagger}) = \lim_{\rho \rightarrow \infty, s \rightarrow \mathbf{M}} \tilde{\theta}^{(\rho,s)} - f(\mathcal{W}^{\parallel\dagger}, \mathcal{W}^{\perp\dagger}),$$

is given by

$$bias(\tilde{\theta} | \mathcal{W}^{\parallel\dagger}, \mathcal{W}^{\perp\dagger}) = g(\mathcal{W}^{\parallel\dagger}) - f(\mathcal{W}^{\parallel\dagger}, \mathcal{W}^{\perp\dagger}).$$

Proof.

$$\begin{aligned} \mathbb{E}[f(\mathcal{W}) | \mathcal{Y}] &= \mathbb{E}\{\mathbb{E}[f(\mathcal{W}) | \mathcal{W}^{\parallel}, \mathcal{Y}^{(\rho,s)}] | \mathcal{Y}^{(\rho,s)}\} \\ &= \mathbb{E}\{\mathbb{E}[f(\mathcal{W}) | \mathcal{W}^{\parallel}] | \mathcal{Y}^{(\rho,s)}\} \\ &= \mathbb{E}\{g(\mathcal{W}^{\parallel}) | \mathcal{Y}^{(\rho,s)}\} \end{aligned}$$

It follows from Property 2 of Definition 2.3 that

$$\mathbb{E}[f(\mathcal{W}) | \mathcal{Y}^{(\rho,s)}] \xrightarrow[\rho \rightarrow \infty, s \rightarrow \mathbf{M}]{a.s.} g(\mathcal{W}^{\parallel\dagger})$$

We therefore have that

$$\begin{aligned}
\text{bias}(\tilde{\theta} | \mathcal{W}^{\parallel\dagger}, \mathcal{W}^{\perp\dagger}) &= \lim_{\rho \rightarrow \infty, s \rightarrow \mathbf{M}} \tilde{\theta}^{(\rho, s)} - f(\mathcal{W}^{\parallel\dagger}, \mathcal{W}^{\perp\dagger}) \\
&= \lim_{\rho \rightarrow \infty, s \rightarrow \mathbf{M}} \mathbb{E}[f(\mathcal{W}) | \mathcal{Y}^{(\rho, s)}] - f(\mathcal{W}^{\parallel\dagger}, \mathcal{W}^{\perp\dagger}) \\
&= g(\mathcal{W}^{\parallel\dagger}) - f(\mathcal{W}^{\parallel\dagger}, \mathcal{W}^{\perp\dagger}).
\end{aligned}$$

□

This bias has an identical functional form to the large sample bias of Bayesian PIMs (Gustafson, 2015). The implication is that, like Bayesian PIMs, scale simulation suffers from a large sample bias: it is the bias induced by using a scale-model in lieu of data that identifies the true scale. Still, the next result shows that this bias is acknowledged by a variance that does not tend to zero even in the asymptotic limit. First, we must provide two results that give context to the next proposition.

Theorem A.4. *Let $\tilde{f} = \mathbb{E}_{p(\mathcal{W}^{\perp} | \mathcal{W}^{\parallel})} f(\mathcal{Y}^{(\rho, s)}, \mathcal{W}^{\perp})$ be a scale simulation estimator with corresponding target estimand $f(\mathcal{W}^{\parallel}, \mathcal{W}^{\perp})$ and measurement model $p(\mathcal{Y}^{(\rho, s)} | \mathcal{W}^{\parallel})$ such that uncertainty in \mathcal{W}^{\parallel} tends to zero as $\rho \rightarrow \infty$ and $s \rightarrow \mathbf{M}$. Then the asymptotic variance of \tilde{f} is given by*

$$\lim_{\rho \rightarrow \infty, s \rightarrow \mathbf{M}} \text{Var}(\tilde{f} | \mathcal{Y}^{(\rho, s)}) \geq \int \left\{ \text{bias}(\tilde{f} | \mathcal{W}^{\parallel\dagger}, \mathcal{W}^{\perp}) \right\}^2 p(\mathcal{W}^{\perp} | \mathcal{W}^{\parallel\dagger}) d\mathcal{W}^{\perp}$$

where $\mathcal{W}^{\parallel\dagger}$ denotes the true value of \mathcal{W}^{\parallel} and

$$\text{bias}(\tilde{f} | \mathcal{W}^{\parallel\dagger}, \mathcal{W}^{\perp}) = E_{p(\mathcal{W}^{\perp} | \mathcal{W}^{\parallel\dagger})} [f(\mathcal{W}^{\parallel\dagger}, \mathcal{W}^{\perp})] - f(\mathcal{W}^{\parallel\dagger}, \mathcal{W}^{\perp}).$$

Proof.

$$\begin{aligned}
\text{Var}(\tilde{\theta} | \mathcal{Y}^{(\rho, s)}) &= \mathbb{E} \{ \text{Var}(f(\mathcal{W}) | \mathcal{W}^{\parallel}, \mathcal{Y}^{(\rho, s)}) | \mathcal{Y}^{(\rho, s)} \} \\
&\quad + \text{Var} \{ \mathbb{E}(f(\mathcal{W}) | \mathcal{W}^{\parallel}, \mathcal{Y}^{(\rho, s)}) | \mathcal{Y}^{(\rho, s)} \} \\
&= \mathbb{E} \{ \text{Var}(f(\mathcal{W}) | \mathcal{W}^{\parallel}) | \mathcal{Y}^{(\rho, s)} \} + \text{Var} \{ \mathbb{E}(f(\mathcal{W}) | \mathcal{W}^{\parallel}) | \mathcal{Y}^{(\rho, s)} \}
\end{aligned}$$

The second term is always greater than or equal to zero implying that

$$\lim_{\rho \rightarrow \infty, s \rightarrow \mathbf{M}} \text{Var}(\tilde{\theta} | \mathcal{Y}^{(\rho, s)}) \geq \mathbb{E} \{ \text{Var}(f(\mathcal{W}) | \mathcal{W}^{\parallel\dagger}) | \mathcal{W}^{\parallel\dagger} \}$$

where we have also used the assumption that $p(\mathcal{Y}^{(\rho,s)}|\mathcal{W}^{\parallel})$ is such that our uncertainty in \mathcal{W}^{\parallel} tends to zero as $\rho \rightarrow \infty$ and $s \rightarrow \mathbf{M}$. It follows that

$$\lim_{\rho \rightarrow \infty, s \rightarrow \mathbf{M}} \text{Var}(\tilde{\theta} | \mathcal{Y}^{(\rho,s)}) \geq \text{Var}(f(\mathcal{W}^{\perp}, \mathcal{W}^{\parallel\dagger}) | \mathcal{W}^{\parallel\dagger}).$$

Based on the definition of variance we then have

$$\lim_{\rho \rightarrow \infty, s \rightarrow \mathbf{M}} \text{Var}(\tilde{\theta} | \mathcal{Y}^{(\rho,s)}) \geq \int \{f(\mathcal{W}^{\parallel\dagger}, \mathcal{W}^{\perp}) - g(\mathcal{W}^{\parallel\dagger})\}^2 p(\mathcal{W}^{\perp} | \mathcal{W}^{\parallel\dagger}) d\mathcal{W}^{\perp}.$$

This is equivalent to

$$\lim_{\rho \rightarrow \infty, s \rightarrow \mathbf{M}} \text{Var}(\tilde{\theta} | \mathcal{Y}^{(\rho,s)}) \geq \int \left\{ \text{bias}(\tilde{\theta} | \mathcal{W}^{\parallel\dagger}, \mathcal{W}^{\perp}) \right\}^2 p(\mathcal{W}^{\perp} | \mathcal{W}^{\parallel\dagger}) d\mathcal{W}^{\perp}.$$

□

Notably, the lower bound is achieved whenever

$$\lim_{\rho \rightarrow \infty, s \rightarrow \mathbf{M}} \text{Var} \{ \mathbb{E}(f(\mathcal{W}) | \mathcal{W}^{\parallel}) | \mathcal{Y}^{(\rho,s)} \} = 0,$$

i.e., when

$$\lim_{\rho \rightarrow \infty, s \rightarrow \mathbf{M}} \text{Var} \{ g(\mathcal{W}^{\parallel}) | \mathcal{Y}^{(\rho,s)} \} = 0.$$

The next two results show two important conditions under which this occurs and the lower bound is achieved.

Lemma A.5. *If $f(\mathcal{W})$ is a scalar target estimand and $p(\mathcal{Y}^{(\rho,s)}|\mathcal{W}^{\parallel})$ is chosen such that our uncertainty in \mathcal{W}^{\parallel} tends to zero as $\rho \rightarrow \infty$ and $s \rightarrow \mathbf{M}$ then*

$$\lim_{\rho \rightarrow \infty, s \rightarrow \mathbf{M}} \text{Var}(g(\mathcal{W}^{\parallel}) | \mathcal{Y}^{(\rho,s)}) = 0.$$

Proof.

$$\text{Var}(g(\mathcal{W}^{\parallel}) | \mathcal{Y}^{(\rho,s)}) = \text{Var}(E[f(\mathcal{W}) | \mathcal{W}^{\parallel}] | \mathcal{Y}^{(\rho,s)})$$

By assumption, in the limit as $\rho \rightarrow \infty$ and $s \rightarrow \mathbf{M}$, our uncertainty in the distribution of \mathcal{W}^{\parallel} goes to zero such that

$$\lim_{\rho \rightarrow \infty, s \rightarrow \mathbf{M}} \text{Var}(E[f(\mathcal{W}) | \mathcal{W}^{\parallel}] | \mathcal{Y}^{(\rho,s)}) = \text{Var}(E[f(\mathcal{W}) | \mathcal{W}^{\parallel}] | \mathcal{W}^{\parallel\dagger})$$

If $f(\mathcal{W})$ is a scalar function then $E[f(\mathcal{W}) | \mathcal{W}^{\parallel}]$ must also be a scalar function, it follows that

$$\text{Var}(E[f(\mathcal{W}) | \mathcal{W}^{\parallel}] | \mathcal{W}^{\parallel\dagger}) = 0.$$

□

Lemma A.6. *If $f(\mathcal{W})$ is a probabilistic model (i.e., $P_\theta(\mathcal{W})$) that is identifiable and $p(\mathcal{Y}^{(\rho,s)}|\mathcal{W}^\parallel)$ is chosen such that our uncertainty in \mathcal{W}^\parallel tends to zero as $\rho \rightarrow \infty$ and $s \rightarrow \mathbf{M}$, then*

$$\lim_{\rho \rightarrow \infty, s \rightarrow \mathbf{M}} \text{Var}(g(\mathcal{W}^\parallel)|\mathcal{Y}^{(\rho,s)}) = 0.$$

Proof. If $f(\mathcal{W}) = P_\theta(\mathcal{W})$ is identifiable, then $E[f(\mathcal{W})|\mathcal{W}^\parallel]$ is a scalar function of \mathcal{W}^\parallel . The rest of the proof follows from Lemma A.5. \square

In short, on the mild assumption that our uncertainty in \mathcal{W}^\parallel tends to zero with infinite data, Lemmas A.5 and A.6 show that as long as the target estimand $f(\mathcal{W})$ is not an unidentified probabilistic model or a degenerate function that the following limiting variance relationship holds

$$\lim_{\rho \rightarrow \infty, s \rightarrow \mathbf{M}} \text{Var}(g(\mathcal{W}^\parallel)|\mathcal{Y}^{(\rho,s)}) = 0.$$

We expect that the use of unidentified probabilistic target estimands and degenerate scalar target estimands will be rare as that would imply that the question of interest is not well posed even in the complete-data setting. We therefore expect that the lower bound variance of Theorem A.4 will be achieved in most use cases.

There are three remarkable conclusions that can be drawn from these results. First, so long as a model for \mathcal{Y} is chosen such our uncertainty in \mathcal{W}^\parallel diminishes to zero in the asymptotic limit (e.g., any standard parametric model), then scale-simulation estimators explicitly acknowledge their bias through their variance. Second, the lower bound variance is of an identical functional form to that of Bayesian PIMs implying that scale simulation estimators are as conservative as Bayesian PIMs, if not moreso. Third, we find that that this lower bound is achieved by scale simulation estimators in so long as the target estimand is not pathologic (i.e., unidentified or degenerate). In short, scale simulation estimators have similar asymptotic properties to Bayesian PIMs while allowing for substantially greater expressive flexibility.

Finally, these results also explain the unacknowledged bias seen with ALDEEx2 or any other model that uses an identifying restriction. If the scale model $p(\mathcal{W}^\perp|\mathcal{W}^\parallel)$ is a point mass, then the asymptotic variance is zero. The relationship between the asymptotic variance and the large sample bias shows that these models do not acknowledge any potential bias introduced through their chosen identifying restriction. Clearly, if there is any uncertainty in that identifying restriction, then, based on the definition of identifying restrictions, these models have an unacknowledged bias with probability 1.

B Simulation and Data Analysis Details

Simulation Details

For all of the simulations, we simulated a data set with 21 taxa across two conditions using multinomial sampling. Sequencing depth was set to 5,000, and, unless otherwise specified, sample size was set to 50 ($n = 50$). ALDEx2 and DESeq2 were fit using their respective Bioconductor packages. For the simulations, default settings were used for each. For ALDEx2, 128 Monte Carlo samples were used, and the t-test with the Benjamini-Hochberg correction were used to find significance. For DESeq2, the Wald test was used, and Benjamini-Hochberg p-values were used to determine significance. Unless otherwise stated, $\alpha = 0.05$.

Further, we extended several of our simulation results, including Figure 1 in the main text to include scale simulation and Figure 2b in the main text to show how inference changes as a function of α . Shown in Supplementary Figure 1a, we find that scale simulation remains calibrated as sample size increases. This is in direct contrast to the results of ALDEx2 and DESeq2. Shown in Supplementary Figure 1b, we find that, like γ , inferred results can vary greatly as a function of the uncertainty in the scale model as expressed through α .

For Figure 3 in the main text and Supplementary Figure 1, we focused on the effect sizes returned by ALDEx2. These effect sizes are calculated as the median standardized differences between conditions (i.e., the median ratio of the difference between conditions and the maximum within condition difference). This metric has an inherent link to Cohen's d (Fernandes et al., 2018). See Fernandes et al. (2014) and Fernandes et al. (2018) for more details.

Real Data Analysis Experiment Details

Bioreactor Culturing

The bioreactor run consisted of 8 continuous-flow vessels (Multifors 2, Infors) cultured over 25 total days according to previously established protocols (Silverman et al., 2018; Letourneau et al., 2021). Briefly, vessels were inoculated with identical inoculum derived from a single healthy stool donor. Vessels were maintained anaerobic under nitrogen, kept at 37 °C, continuously stirred

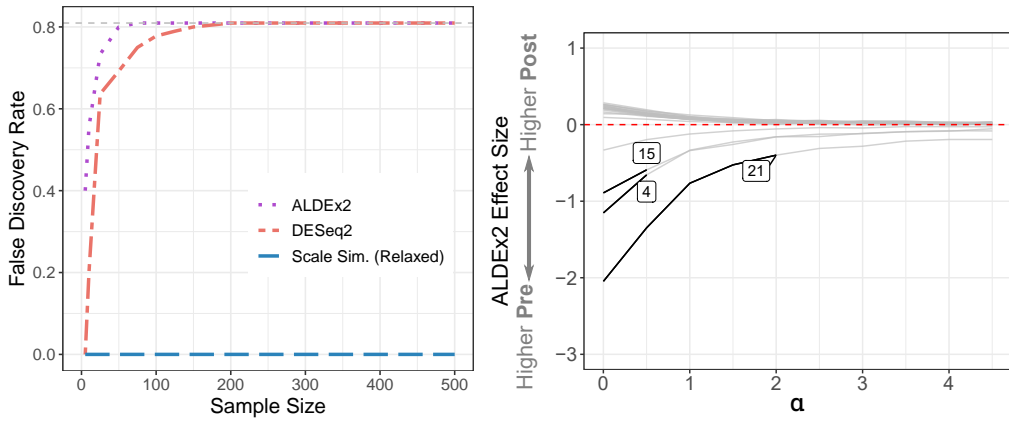


Figure 1: (Left) False discovery rate versus sample size for ALDEEx2, DESeq2, and Scale Simulation (Relaxed Model) for the simulated data. For ALDEEx2 and DESeq2, false discovery rate increases in the presence of infinite data. In contrast, Scale Simulation remains calibrated. (Right) Sensitivity analysis showing the estimated ALDEEx2 effect size for each taxa under the Relaxed model as a function of α with $\gamma = 0.20$. A black line signifies that the estimated effect size was statistically different from zero with 95% certainty.

at 100 rpm using magnetic impeller stir-shafts, and the total volume of media (400 mL modified Gifu Anaerobic Medium) was turned over once per 24 hours. Samples for sequencing and flow cytometry were collected daily at 4pm by syringe via a sterilized sampling port. Since the volume of each vessel remained fixed at 400 mL, concentration of cells is directly proportional to absolute abundance.

Cell Quantification by Flow Cytometry

Samples were serially diluted ten-fold for a final dilution of 1:1000. Serial dilutions were performed in PBS, with the final dilution performed into wells of a 96-well plate containing PBS with 1 μ L SYBR green/DMSO (1:499 SYBR:DMSO) per 180 μ L total volume. The final 200 μ L mixture including sample and SYBR green was incubated 15 min at 37 °C (Vandeputte et al., 2017).

Flow cytometry was performed using a MACSQuant Flow Cytometer (Miltenyi Biotec). The 96-well plate containing samples was maintained on a chill rack for the duration of the run. 10 μ L was taken for measurement. Forward scatter, side scatter, and SYBR fluorescence (using channel B1, log5, 274 V) were recorded.

Flow cytometry data was analyzed in FlowJo using a two-step gating strategy. A single sample containing cells but no SYBR was used to develop gates which were then applied to all samples. First, using a graph of forward scatter vs. side scatter, we roughly selected for the center of point density, omitting extreme values (i.e. possibly representing cellular debris and/or particle aggregates). Second, examining the SYBR channel, we excluded counts that fell within the range of the no-SYBR control.

16S rRNA-Gene Encoding Amplicon Sequencing

16S rRNA gene amplicon sequencing was performed as previously described using custom barcoded primers targeting the V4 region of the gene, resulting in 150 bp paired-end reads sequenced by Illumina MiniSeq according to previously published protocols (Silverman et al., 2018; Letourneau et al., 2021). DADA2 was used to identify and quantify sequence variants (SVs) in our dataset, using version 123 of the Silva database. Taxa that had counts of less than 2,500 across all samples were filtered and amalgamated into a separate category.

Data Analysis

For our analysis, we restricted ourselves to days 1 and 14. Furthermore, we used data from vessels 3, 4, 5, 6, 7, and 8 only due to limitations in the data. We noted a difference between flow cytometry concentrations between days regardless of vessel. See Figure 2 for details.

We tested a model of differential expression including indicator terms for each vessel and day. For ALDEx2, we used the generalized linear model test with 250 Monte Carlo Samples. We assessed differential expressed taxa based on the p-values ($\alpha = 0.05$) for day alone. For DESeq2, we employed the likelihood ratio test with a reduced model containing only the vessel and assessed differential abundance using the same criteria as ALDEx2.

Eleven different sequence variants were declared significant by at least one method. Taxonomic information for these significant sequence variants is presented in Table 1.

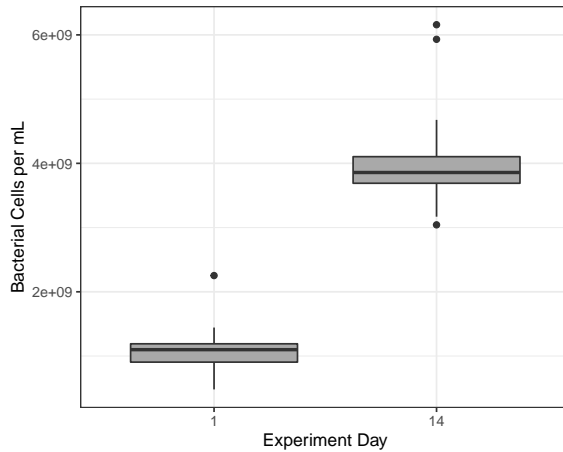


Figure 2: Variation of flow cytometry data by day. Note that there was a higher concentration of cells on day 14 regardless of vessel. This has biological validity based on the experimental goals of the study.

Table 1: Taxonomic information of significant sequence variants identified in the Real Data Analysis.

| Sequence | Taxonomic Information |
|----------|-------------------------------------|
| 1 | <i>Bacteroides spp.</i> |
| 3 | <i>Bacteroides uniformis</i> |
| 4 | <i>Peptoniphilus spp.</i> |
| 5 | <i>Pyramidobacter piscolens</i> |
| 9 | <i>Streptococcus spp.</i> |
| 10 | <i>Anaerosalibacter bizertensis</i> |
| 16 | <i>Dorea formicigenerans</i> |
| 25 | <i>Flavonifractor plautii</i> |
| 27 | <i>Parabacteroides merdae</i> |
| 28 | <i>Anaerococcus vaginalis</i> |
| 31 | <i>Anaerostipes hadrus</i> |

C Derivation of Relative and Scale Distributions for Scale Simulation

C.1 Derivation of Conditional Relative Model

Recall that the target model is:

$$Y_j \sim \text{Mult}(\mathcal{W}_j^{\parallel}) \quad (2)$$

$$\mathcal{W}_j = \mathcal{W}_j^{\perp} \mathcal{W}_j^{\parallel} \quad (3)$$

$$\mathcal{W}_j = \exp(\psi_j) \quad (4)$$

$$\psi_j \sim N(BX, \Omega, I) \quad (5)$$

$$B \sim N(M, \Omega, \Gamma) \quad (6)$$

$$\Omega \sim IW(\nu, \Xi) \quad (7)$$

First, we defined G as a linear map:

$$G = \begin{bmatrix} F \\ H \end{bmatrix} \quad (8)$$

where $F = [I_{D-1}, -\mathbf{1}_{D-1}]$ and $H = \mathbf{1}_D$. Note that for any arbitrary vector θ and matrix Σ , we have:

$$G\theta = \begin{bmatrix} F\theta \\ G\theta \end{bmatrix} = \begin{bmatrix} \theta^{\parallel} \\ \theta^{\perp} \end{bmatrix} \quad (9)$$

$$G\Sigma = G\Sigma G^T = \begin{bmatrix} F\Sigma F^T & F\Sigma H^T \\ H\Sigma F^T & H\Sigma H^T \end{bmatrix} = \begin{bmatrix} \Sigma^{\parallel} & \Sigma^{+T} \\ \Sigma^{+} & \Sigma^{\perp} \end{bmatrix} \quad (10)$$

where the \parallel and \perp notation follows the rest of the paper.

Applying G to ψ from the model defined in Equations 2-7:

$$G\psi = \begin{bmatrix} \psi^{\parallel} \\ \psi^{\perp} \end{bmatrix} \quad (11)$$

Since it is an affine transformation, we get (Theorem 2.3.10, Gupta and Nagar (2000) , page 64):

$$\begin{bmatrix} \psi^{\parallel} \\ \psi^{\perp} \end{bmatrix} \sim N(GBX, G\Omega G^T, I) \quad (12)$$

$$\begin{bmatrix} \psi^{\parallel} \\ \psi^{\perp} \end{bmatrix} \sim N\left(\begin{bmatrix} B^{\parallel} \\ B^{\perp} \end{bmatrix} X, \begin{bmatrix} \Omega^{\parallel} & \Omega^{+T} \\ \Omega^{+} & \Omega^{\perp} \end{bmatrix}, I\right) \quad (13)$$

$$\begin{bmatrix} \psi^{\parallel} \\ \psi^{\perp} \end{bmatrix} \sim N\left(\begin{bmatrix} B^{\parallel} \\ B^{\perp} \end{bmatrix} X, \Omega^*, I\right) \quad (14)$$

from the properties discussed before. Now, we need to marginalize out B and Ω . Starting with B , we can write Equation 14 as:

$$\begin{bmatrix} \psi^{\parallel} \\ \psi^{\perp} \end{bmatrix} = \begin{bmatrix} B^{\parallel} \\ B^{\perp} \end{bmatrix} X + E^B, \quad E^B \sim N(0, \Omega^*, I) \quad (15)$$

Similarly, since $B \sim N(M, \Omega, I)$, by Theorem 2.3.10 (Gupta and Nagar (2000), page 64), we get:

$$GB = \begin{bmatrix} B^{\parallel} \\ B^{\perp} \end{bmatrix} \sim N\left(\begin{bmatrix} M^{\parallel} \\ M^{\perp} \end{bmatrix}, \Omega^*, \Gamma\right) \quad (16)$$

Then, we can write:

$$\begin{bmatrix} B^{\parallel} \\ B^{\perp} \end{bmatrix} = \begin{bmatrix} M^{\parallel} \\ M^{\perp} \end{bmatrix} + E^*, \quad E^* \sim N(0, \Omega^*, \Gamma). \quad (17)$$

This implies that

$$\begin{bmatrix} \psi^{\parallel} \\ \psi^{\perp} \end{bmatrix} = \left(\begin{bmatrix} M^{\parallel} \\ M^{\perp} \end{bmatrix} + E^* \right) X + E^B \quad (18)$$

$$= \begin{bmatrix} M^{\parallel} \\ M^{\perp} \end{bmatrix} X + E^* X + E^B \quad (19)$$

where E^B and E^* are defined as before. Using Theorem 2.3.10 (Gupta and Nagar (2000), page 64), the distribution of $E^* X$ is:

$$E^* X \sim N(0, \Omega^*, X^T \Gamma X) \quad (20)$$

Then, by Gupta and Nagar (2000) (page 82), we get

$$\begin{bmatrix} \psi^{\parallel} \\ \psi^{\perp} \end{bmatrix} \sim N \left(\begin{bmatrix} M^{\parallel} \\ M^{\perp} \end{bmatrix} X, \Omega^*, I + X^T \Gamma X \right) \quad (21)$$

To marginalize out Ω^* , we start by applying G to Ω :

$$G \Omega G^T = \Omega^* \sim \text{IW}(\nu, \Xi^*) \quad (22)$$

where $\Xi^* = G \Xi G^T = \begin{bmatrix} \Xi^{\parallel} & \Xi^{+T} \\ \Xi^+ & \Xi^{\perp} \end{bmatrix}$. Let $\hat{E} \sim N(0, I, I + X^T \Gamma X)$. This implies that (Theorem 4.2.1 of Gupta and Nagar (2000), page 134)

$$\Omega^{-1} \hat{E} + \begin{bmatrix} M^{\parallel} \\ M^{\perp} \end{bmatrix} X \sim T \left(\nu, \begin{bmatrix} M^{\parallel} \\ M^{\perp} \end{bmatrix} X, \Xi^*, I + X^T \Gamma X \right) \quad (23)$$

which implies

$$\begin{bmatrix} \psi^{\parallel} \\ \psi^{\perp} \end{bmatrix} \sim T \left(\nu, \begin{bmatrix} M^{\parallel} \\ M^{\perp} \end{bmatrix} X, \Xi^*, I + X^T \Gamma X \right). \quad (24)$$

From Gupta and Nagar (2000) (page 163), the marginal distribution of ψ^{\parallel} is:

$$\psi^{\parallel} \sim T(\nu, M^{\parallel} X, \Xi^{\parallel}, I + X^T \Gamma X) \quad (25)$$

which implies the model for $\psi^{\parallel} | Y$ is:

$$Y_j \sim \text{Mult}(\mathcal{W}_j^{\parallel}) \quad (26)$$

$$\psi^{\parallel} \sim \text{ALR}_D(\mathcal{W}^{\parallel}) \quad (27)$$

$$\psi^{\parallel} \sim T(\nu, M^{\parallel} X, \Xi^{\parallel}, I + X^T \Gamma X). \quad (28)$$

where $ALR(\cdot)$ denotes the additive log-ratio transform. Note that this is exactly the collapse sampler from Silverman et al. (2022).

C.2 Derivation of Implied Scale Model for Bayesian PIM

Recall from the previous section:

$$\begin{bmatrix} \psi^{\parallel} \\ \psi^{\perp} \end{bmatrix} \sim T \left(\nu, \begin{bmatrix} M^{\parallel} \\ M^{\perp} \end{bmatrix} X, \Xi^*, I + X^T \Gamma X \right). \quad (29)$$

Then, from Gupta and Nagar (2000) (page 163), the distribution of $\psi^{\perp} | \psi^{\parallel}$ is a multivariate T-distribution:

$$\psi^{\perp} | \psi^{\parallel} \sim T[\nu + D, M^{\perp} X + (\Xi^+)^T (\Xi^{\parallel})^{-1} (\psi^{\parallel} - M^{\parallel} X)], \quad (30)$$

$$\Xi_{22.1}, (I + X^T \Gamma X) (I + (I + X^T \Gamma X)^{-1} (\psi^{\parallel} - M^{\parallel} X)^T (\Xi^{\parallel})^{-1} (\psi^{\parallel} - M^{\parallel} X)) \quad (31)$$

where $\Xi_{22.1} = \Xi^{\perp} - (\Xi^+)(\Xi^{\parallel})^{-1}(\Xi^+)^T$.

C.3 Derivation of Conditional Model for Parameters

For the model of $P(B, \Omega | \psi_j = \psi_j^{\parallel} \psi_j^{\perp}, X, Y)$. Note that

$$P(B, \Omega | \psi_j, X, Y) = P(B, \Omega | \psi_j, X) \quad (32)$$

$$= P(B | \Omega, \psi_j, X) P(\Omega | \psi_j, X) \quad (33)$$

which denotes a multivariate conjugate linear model that can be efficiently sampled according to (Rossi et al., 2012):

$$\begin{aligned} \nu_N &= \nu + N \\ \Gamma_N &= (X X^T + \Gamma^{-1})^{-1} \\ B_N &= (\psi X^T + M \Gamma^{-1}) \Gamma_N \\ \Xi_N &= \Xi(\psi - B_N X) (\psi - B_N X)^T + (B_N - M) \Gamma^{-1} (B_N - M)^T \\ p(\Omega | \psi, X) &= \text{IW}(\Xi_N, \nu_N) \\ p(B | \Omega, \psi, X) &= N(B_N, \Omega, \Gamma_N) \end{aligned}$$

which is the uncollapse sampler from Silverman et al. (2022).

C.4 Collapse-Uncollapse Sampling Details

While conceptually straightforward, scale simulation requires efficient sampling for three separate stages: a compositional model, a scale model, and an inferential model. For the case of the multinomial logistic normal model, our sampling details closely mimic the Collapse-Uncollapse (CU) sampler of Silverman et al. (2022). Intuitively, the basic sampler follows three steps:

1. Sample from the partially identified base scale model $P(\mathcal{W}^{\parallel}|\mathcal{Y})$.
2. Sample from the scale model $P(\mathcal{W}^{\perp}|\mathcal{W}^{\parallel})$.
3. Sample from the target model $P(B, \Omega|\psi = \exp(\mathcal{W}^{\parallel}\mathcal{W}^{\perp}))$.

Sampling from the scale model is typically efficient as it is low-dimension and flexible. To date, efficient routines for these models are already implemented in R.

However, sampling from Steps 1 and 3 are cumbersome but were recently made much more efficient and scalable by Silverman et al. (2022). Their approach relies on rewriting the above multinomial logistic-normal model as a marginally latent matrix-t process. Then, they develop efficient inference for this class of models using a Collapse-Uncollapse (CU) sampling approach. Such an approach vastly improves computational efficiency, increasing the usability of these models to much larger sequence count data sets. See Silverman et al. (2022) for complete details on implementation.

We utilize the logic behind the CU sampler to infer Steps 1 and 3. These routines are efficiently implemented in the R package `fido` (Silverman et al., 2022). Slight modifications are necessary as Silverman et al. (2022) presents a multinomial logistic-normal model. Formal implementation details for scale

simulation are outlined in Algorithm 1.

Algorithm 1: Modified Collapse–Uncollapse Sampler for Scale Simulation

Data: Y

Result: S samples of the form $\{B^{(s)}, \Omega^{(s)}\}$

Sample $\{\mathcal{W}^{\parallel(1)}, \dots, \mathcal{W}^{\parallel(s)}\} \sim P(\mathcal{W}^{\parallel} | Y)$ using the Collapse sampler of Silverman et al. (2022);

Sample $\{\mathcal{W}^{\perp(1)}, \dots, \mathcal{W}^{\perp(s)}\} \sim P(\mathcal{W}^{\perp} | \mathcal{W}^{\parallel})$;

do in parallel

 | Sample $\{(B^{(1)}, \Omega^{(1)}), \dots, (B^{(s)}, \Omega^{(s)})\} \sim P(B, \Omega | \psi = \exp(\mathcal{W}^{\perp} \mathcal{W}^{\parallel}))$
 | using the Uncollapse sampler of Silverman et al. (2022);

end

D Additional Data Simulations

D.1 Sample Size Analysis for Real Data Experiment

To show that ALDEx2 and DESeq2 suffer from unacknowledged bias, we conducted a simple experiment on our real data to understand how behavior across methods would change as sample size increased. To do so, we randomly sampled vessels from the six available vessels in the real data to create the desired number of “new” vessels. For each of these subsampled vessels, we used multinomial resampling to create the observed counts on Day 1 and Day 14. From there, we fit a model analogous to that presented in the manuscript. We included indicator variables for each vessel and well as day. We fit ALDEx2, DESeq2, and scale simulation with the designed-based scale model and recorded the number of false discoveries for each method. This was repeated 10 times for each sample size. Results are shown in Figure 3. As the number of vessels increase, FDR rapidly increases for ALDEx2 and DESeq2. In contrast, scale simulation remains calibrated.

D.2 DESeq2 Bias and Variance

Here, we demonstrate that DESeq2’s imputation of the system scale in Section 6.1 is highly accurate (low bias) but still has even lower variance leading to an unacknowledged bias and the elevated false discovery rates described in that section. As discussed in the main text, DESeq2’s median of ratios

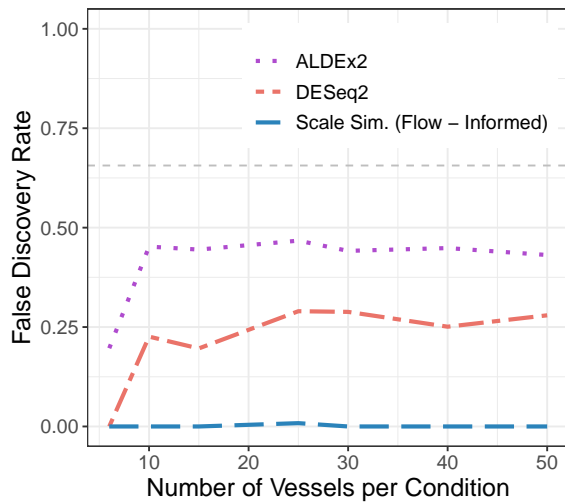


Figure 3: Mean false discovery rate by method for resampling experiment over 10 replicates. For each replicate, vessels were randomly sampled from the six available in the experiment. Data was created for each sample by Multinomial sampling using the original data as weights. The maximum false discovery rate was approximately 0.65.

normalization is an identifying restriction and therefore implies infinite certainty in the unmeasured system scale. Still, Figure 1 demonstrates that in the finite sample regime, DESeq2’s negative binomial sampling model introduces uncertainty into the estimates that can buffer against false positives. Therefore, to study the bias and variance of the DESeq2 estimator applied to a particular dataset we find it most appropriate to consider the *effective scale model*, the scale model implied by DESeq2’s actual scale model (which arises from the median of ratios normalization) combined with the sampling variation of the negative binomial model.

We quantify DESeq2’s effective scale model as follows. DESeq2 estimates expected log-fold changes θ_i which can be written as

$$\theta_i = \mathbb{E} \left[\log \frac{W_{i(case)}^{\parallel}}{W_{i(control)}^{\parallel}} \right] + \mathbb{E} \left[\log \frac{W_{i(case)}^{\perp}}{W_{i(control)}^{\perp}} \right] \quad (34)$$

$$= \theta_i^{\parallel} + \theta_i^{\perp}. \quad (35)$$

DESeq2 also provides standard error of its estimates which allow us to approximate the sampling distribution of its estimates as $P(\hat{\theta}_i) = N(\hat{\theta}_i, \sigma^2(\hat{\theta}_i))$ where $\sigma(\hat{\theta}_i)$ denotes the standard error of the estimate θ_i . With this notation we can denote the effective scale model of DESeq2 as $P(\hat{\theta}^{\perp})$. Note that for any estimate $\hat{\theta}$ we can identify $\hat{\theta}^{\parallel}$ with

$$\hat{\theta}_i^{\parallel} = \hat{\theta}_i - \text{mean}(\hat{\theta}_1, \dots, \hat{\theta}_D). \quad (36)$$

Therefore, we have the following algorithm to sample from the effective scale model of DESeq2. Repeatedly sample from the approximated scale model $P(\hat{\theta})$ and then transform those samples using Equation (36) into samples from $P(\hat{\theta}^{\perp})$.

Applying this algorithm to the DESeq2 estimates in Section 6.1 allowed us to estimate the effective scale model of DESeq2 shown in Figure 4. Most of the probability mass of this scale model lies between -0.16 and -0.12. This corresponds to an assumption (with $> 95\%$ certainty) that the total microbial load in the post-antibiotic condition is between 85.2% and 86.9% of the pre-antibiotic load. Remarkably this is just a 2% error relative to the true simulated value (red line). Still, we see that the DESeq2 model overestimates its certainty in this estimate of θ^{\perp} which represents an unacknowledged bias and leads to the high false discovery rate seen in Figure 2 of the main text. Together, these results demonstrate that even a model with small bias in

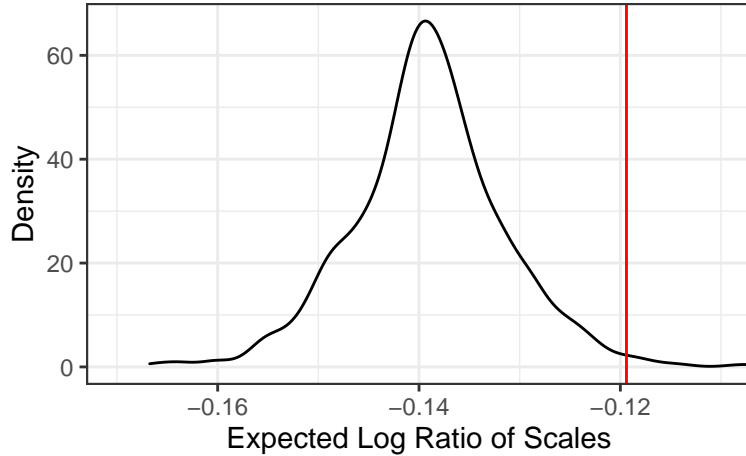


Figure 4: Kernel Density Estimate for the Effective Scale Model of DESeq2 from Section 6.1 (black line). The simulated value of the expected log ratio of scale is denoted by the red vertical line.

its estimates of scale can still lead to spurious conclusions if its certainty in those estimates is improperly calibrated.

D.3 Bayesian PIM Results

To understand the performance of Bayesian PIM, we fit our scale simulation technique using scale model implied in Section C.2. We compared this model to the results from the gold standard model discussed in the main text. In general, the Bayesian PIM performed well. Then sensitivity and specificity were 72.7% and 95.3%, respectively.

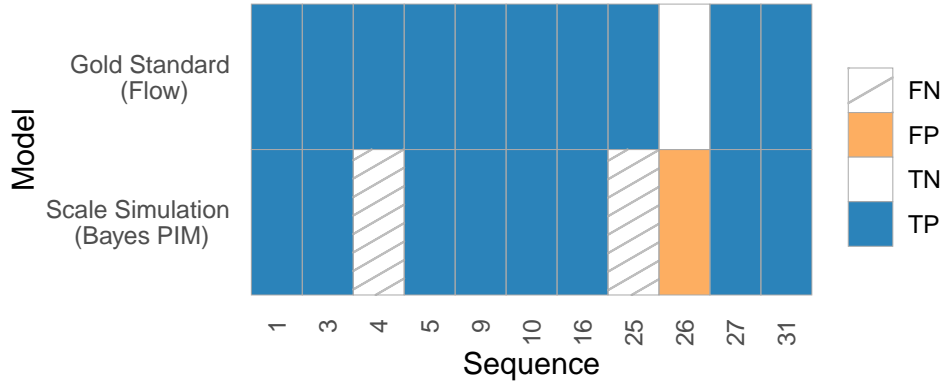


Figure 5: Differential expressed sequences on the real data analysis for the gold standard model (top) and Bayesian PIM (bottom).

References

Fernandes, A. D., Reid, J. N., Macklaim, J. M., McMurrough, T. A., Edgell, D. R., and Gloor, G. B. (2014). Unifying the analysis of high-throughput sequencing datasets: characterizing RNA-seq, 16S rRNA gene sequencing and selective growth experiments by compositional data analysis. *Microbiome*, 2(1):1–13.

Fernandes, A. D., Vu, M. T., Edward, L.-M., Macklaim, J. M., and Gloor, G. B. (2018). A reproducible effect size is more useful than an irreproducible hypothesis test to analyze high throughput sequencing datasets. *arXiv preprint arXiv:1809.02623*.

Friedman, J. and Alm, E. J. (2012). Inferring correlation networks from genomic survey data. *PLoS Computational Biology*, 8(9):e1002687.

Gabrielsen, A. (1978). Consistency and identifiability. *Journal of Econometrics*, 8(2):261–263.

Gupta, A. and Nagar, D. (2000). *Matrix Variate Distributions*. Chapman & Hall/CRC.

Gustafson, P. (2015). *Bayesian inference for partially identified models: Exploring the limits of limited data*, volume 140. CRC Press.

Letourneau, J., Holmes, Z. C., Dallow, E. P., Durand, H. K., Jiang, S., Gupta, S. K., Mincey, A. C., Muehlbauer, M. J., Bain, J. R., and David, L. A. (2021). Ecological memory of prior nutrient exposure in the human gut microbiome. *bioRxiv*.

Rossi, P. E., Allenby, G. M., and McCulloch, R. (2012). *Bayesian statistics and marketing*. John Wiley & Sons.

Silverman, J. D., Durand, H. K., Bloom, R. J., Mukherjee, S., and David, L. A. (2018). Dynamic linear models guide design and analysis of microbiota studies within artificial human guts. *Microbiome*, 6(1):1–20.

Silverman, J. D., Roche, K., Holmes, Z. C., David, L. A., and Mukherjee, S. (2022). Bayesian multinomial logistic normal models through marginally latent matrix-t processes. *Journal of Machine Learning Research*, 23(7):1–42.

Vandeputte, D., Kathagen, G., D’hoe, K., Vieira-Silva, S., Valles-Colomer, M., Sabino, J., Wang, J., Tito, R. Y., De Commer, L., Darzi, Y., et al. (2017). Quantitative microbiome profiling links gut community variation to microbial load. *Nature*, 551(7681):507–511.